

UCSF

UC San Francisco Electronic Theses and Dissertations

Title

The Chlamydia trachomatis Inc Tri1 interacts with the host protein TRAF7 to modulate TRAF7-dependent interactions.

Permalink

<https://escholarship.org/uc/item/43b2v95t>

Author

Herrera, Clara Maria

Publication Date

2024

Peer reviewed|Thesis/dissertation

The Chlamydia trachomatis Inc Tri1 interacts with the host protein TRAF7 to modulate TRAF7-dependent interactions.

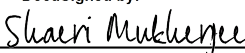
by
Clara M Herrera

DISSERTATION
Submitted in partial satisfaction of the requirements for degree of
DOCTOR OF PHILOSOPHY

in
Biochemistry and Molecular Biology

in the
GRADUATE DIVISION
of the
UNIVERSITY OF CALIFORNIA, SAN FRANCISCO

Approved:

DocuSigned by:

7AA908684B40471... Shaeri Mukherjee
Chair

DocuSigned by:

DocuSigned by:4E5... Joanne Engel


DocuSigned by: Anita Sil

DocuSigned by:

B39DA64A208E4CB... David Toczyski

Committee Members

Copyright 2024

by

Clara Herrera

Para mi madre.

Thank you for always believing in me.

ACKNOWLEDGEMENTS

I never would have finished this PhD without the support of so many people. I would like to thank Joanne for her mentorship and for dedicating countless weekends to making sure this work was finished. The Engel lab was a second home for me, and I'm so thankful for all the lab members past and present who got me through these years. Thank you to the chlam fam (Jess, Cheri, Khavong, Kate) and pseudbrood (Ramiro, Henriette, Yuki) for being a source of joy and being willing to talk about anything. Thank you to the 4th floor labs and the community you have created. Thank you to Rick and the UCSF boxing crew for keeping me sane and making me laugh when I needed it the most. Thank you to Sarah and Michael for your friendship and for always being willing to try new things with me. Thank you to Fatema and Jaimee for everything, but especially for insisting on helping me move out of my apartment because sometimes I am very bad at planning. Finally, I would like to thank my family, and my mom, dad, and aunt especially, for being a constant source of unconditional support.

STATEMENT REGARDING AUTHOR CONTRIBUTIONS

Chapter 2 is the draft of a manuscript intended for publication and submitted to BioRxiv: The *Chlamydia trachomatis* Inc Tri1 interacts with TRAF7 to displace native TRAF7 interacting partners. Clara M. Herrera, Eleanor McMahon, Danielle L. Swaney, Jessica Sherry, Khavong Pha, Kathleen Adams-Boone, Jeffrey R. Johnson, Nevan J. Krogan, Meredith Stevers, David Solomon, Cherilyn Elwell, Joanne Engel.

I, Clara Herrera, designed and conducted experiments under the guidance of Joanne Engel. Samples for affinity purification-mass spectrometry of infected cells were prepared by Eleanor McMahon and Jessica Sherry, run by Jeffrey Johnson, and analyzed by Danielle Swaney. Samples for TRAF7 affinity purification-mass spectrometry were run and analyzed by Danielle Swaney.

Chapter 3 is unpublished work related to the full TRAF7 affinity purification-mass spectrometry dataset (introduced in Chapter 2) run and analyzed by Danielle Swaney and Merve Cakir.

Chapter 4 is unpublished work conducted using RNA-sequencing of cells infected with a Tri1 CRISPRi KD strain. Cell lysates from infected cells were prepared by me. Padmini Deosthale and Ryan Ward prepared libraries and conducted RNAseq experiments and Hoang Van Phan conducted additional bioinformatic analysis under the supervision of Chaz Langelier. Tri1 CRISPRi strains were generated and provided by Natalie Sturd, Elizabeth Rucks, and Scot Ouellette.

The *Chlamydia trachomatis* Inc Tri1 interacts with the host protein TRAF7 to modulate TRAF7-dependent interactions.

Clara Herrera

ABSTRACT

Like any successful intracellular pathogen, *Chlamydia trachomatis* must overcome several host defenses to complete its developmental cycle. *Chlamydia* is thought to accomplish this through the employment of effector proteins, particularly a unique class of effectors which are inserted in the *Chlamydial* inclusion membrane. To test the hypothesis that these inclusion membrane proteins (Incs) target host cell proteins, our lab conducted an affinity purification-mass spectrometry screen (AP-MS) in which cells were transfected with individually tagged Incs. The predicted interaction between the Inc Tri1 and the host ubiquitin ligase TRAF7 is the subject of this work.

In this dissertation, we characterize the Tri:TRAF7 complex during infection and reveal that Tri1 can disrupt native TRAF7 protein-protein interactions (PPIs, Chapter 2). Through additional analysis of this TRAF7 interactome dataset, we revealed that Tri1 can also promote novel TRAF7 PPIs (Chapter 3). Finally, we conducted RNAseq analysis to determine the role of Tri1 during infection and determined that it may play a modest role in altering signaling pathways. Overall, this work contributes to the growing literature on *C. trachomatis* Incs and highlights the important roles they may play during infection.

TABLE OF CONTENTS

CHAPTER 1 INTRODUCTION	1
REFERENCES.....	6
CHAPTER 2 THE <i>CHLAMYDIA TRACHOMATIS</i> INC TRI1 INTERACTS WITH TRAF7 TO DISPLACE NATIVE TRAF7 INTERACTING PARTNERS.....	10
SUMMARY.....	11
INTRODUCTION.....	12
RESULTS.....	15
DISCUSSION	21
MATERIALS AND METHODS.....	25
ACKNOWLEDGEMENTS.....	32
REFERENCES.....	34
CHAPTER 3 TRI1 ALTERS TRAF7 PROTEIN-PROTEIN INTERACTIONS.....	51
SUMMARY.....	52
INTRODUCTION.....	53
RESULTS.....	54
DISCUSSION	61
MATERIALS AND METHODS.....	62
ACKNOWLEDGEMENTS.....	62
REFERENCES.....	63
CHAPTER 4 SELECT SIGNALING PATHWAYS ARE DEPENDENT ON TRI1 EXPRESSION DURING INFECTION	65
INTRODUCTION.....	66
RESULTS.....	67
DISCUSSION	70
MATERIALS AND METHODS.....	71

ACKNOWLEDGEMENTS.....	74
REFERENCES.....	75
CHAPTER 5 CONCLUSIONS	77

LIST OF FIGURES

CHAPTER 2

FIGURE 2.1. TRI1 AND TRAF7 INTERACT DURING INFECTION	44
FIGURE 2.2. TRAF7 IS RECRUITED TO THE INCLUSION	45
FIGURE 2. 3. THE COILED-COIL DOMAIN OF TRI1 INTERACTS WITH TRAF7	46
FIGURE 2. 4. THE WD40 OF TRAF7 IS NECESSARY AND SUFFICIENT TO INTERACT WITH TRI1	47
FIGURE 2.5. TRI1 DISPLACES MEKK2 AND MEKK3 BINDING TO TRAF7	48
FIGURE S2. 1. ALIGNMENT OF TRI1 FROM L2 SEROVAR D	49
FIGURE S2.2. TRAF7 ANTIBODY DETECTS ENDOGENOUS TRAF7 AND ECTOPICALLY EXPRESSED TRAF7	50

CHAPTER 3

FIGURE 3. 1. TRI1 AND TRAF7 CO-LOCALIZE AT PUNCTA DURING TRANSFECTION	56
FIGURE 3. 2. TRI1 IS PREDICTED TO MODULATE TRAF7 PROTEIN-PROTEIN INTERACTIONS	57
FIGURE 3. 3. TRI1 IS PREDICTED TO PROMOTE TRAF7 INTERACTIONS WITH TRANSPORTER PROTEINS DURING INFECTION	59
FIGURE 3. 4. IPO5 IS RECRUITED TO THE INCLUSION IN A TRI1-DEPENDENT MANNER	60

CHAPTER 4

FIGURE 4. 1. OPTIMIZATION OF RNASEQ CONDITIONS.	68
FIGURE 4. 2. GSEA OF RNASEQ RESULTS IDENTIFIES TRI1-DEPENDENT PATHWAYS DURING INFECTION	69

CHAPTER 1

INTRODUCTION

All successful intracellular pathogens must overcome multiple host cell mechanisms of surveillance to survive. Generally, these organisms display pathogen-associated molecular patterns (PAMPs), which are detected by host pattern recognition receptors (PRRs)(1). Examples of this include cell autonomous signaling mechanisms such as the cGAS/STING pathway, which can detect foreign DNA from pathogens to promote pro-inflammatory pathways and consequently pathogen destruction(2). To counteract these host defense mechanisms, pathogens have evolved sophisticated mechanisms to manipulate or evade host cells processes. Many pathogens secrete proteins into the host cell cytosol, called effectors, to perform these functions. For example, intracellular pathogens such as *Salmonella*, *Yersinia*, and *Legionella*, reprogram host protein ubiquitination, either by regulating host ubiquitin ligases or encoding bacterial ubiquitin ligases(3). Additionally, pathogens may camouflage themselves by replicating within membrane-bound compartments decorated with host lipids that serve to both disguise the pathogen and to prevent the leakage of its DNA into the host cytosol, where it may be recognized by the host innate immune response(4). While membrane-bound pathogens such as *Chlamydia trachomatis* (*C. trachomatis*) and *Toxoplasma gondii* (*T. gondii*) enjoy this additional level of protection from its host, these vacuoles may still be recognized as non-self structures by the host(4–6). If primed for pro-inflammatory signaling by PAMPs, host cells may ubiquitinate pathogenic vacuoles and subsequently recruit adaptor proteins to the vacuole for autophagosomal degradation(4–6). Thus, pathogens must carefully balance their replication with host defenses.

In this work, we focus on the intracellular development of *Chlamydia trachomatis*. *C. trachomatis* is a pathogen of global interest due to its status as the leading bacterial cause of sexually transmitted infections and infectious blindness, with 128.5 million new infections in 2020(7). Additionally, *C. trachomatis* infections are often asymptomatic and may result in sequelae such as pelvic inflammatory disease and infertility if left untreated(8).

C. trachomatis is an obligate intracellular pathogen and is thus tasked with overcoming cellular surveillance mechanisms to complete its developmental cycle(9). *Chlamydia* development occurs as a biphasic cycle. The bacterium first enters cells as an elementary body (EB), transitions into its replicative reticulate body (RB) form, avoids lysosomal detection, and replicates within a membrane-bound compartment termed the inclusion. *Chlamydia* acquires essential nutrients, avoids intracellular detection, and transitions back to its infectious EB form prior to exiting host cells(9). *Chlamydia* is thought to accomplish these feats in by employing a specialized needle-like protein export apparatus, the type III secretion system to insert effectors into either the host cytosol (conventional effectors) or into its own inclusion membrane (inclusion membrane proteins (Incs))(10)). Characterization of the Incs, which are unique to the order *Chlamydiales*, has been limited by their lack of identifiable features through bio- informatic analysis and a past dearth of successful genetic tools in *Chlamydia*(11, 12).

While divergent in sequence, Incs are characterized by the presence of two or more transmembrane domains, with their N- and C-terminal domains extending into the host cell cytosol (12, 13). Thus, Incs are ideally positioned at the host-pathogen interface to interact with host cell proteins. Incs may serve several strategic functions, such as

recruiting host proteins or organelles to the inclusion, disrupting host protein- protein interactions, and/or functioning as scaffolds to generate novel protein-protein interactions at the inclusion(9). Previous studies on Incs have revealed that they can disrupt native protein-protein interactions (9, 14, 15) and evade cell autonomous signaling pathways such as the STING pathway (16). However, the function of most of the *C. trachomatis* Incs remains to be elucidated. To gain insight into the function of Incs, our lab previously used a high through- put proteomics strategy in which we employed affinity purification-mass spectrometry (AP-MS) using epitope-tagged Incs transfected into human cells to identify their host binding partners(17). This study identified at least one predicted high confidence host protein interaction for 2/3 of the *C. trachomatis* serovar D incs. In this dissertation, I focused on the predicted high confidence interaction between the Inc CT224 and the host ubiquitin ligase TRAF7. Little is known about CT224, and its further study thus presented an opportunity to further characterize the functions of Incs. The host protein TRAF7 is a member of the tumor necrosis receptor associated factor (TRAF) family of proteins, which have diverse roles in major immune signaling pathways(18, 19). TRAF7 has reported roles in modulating pro-inflammatory signaling pathways which are relevant for *C. trachomatis* infection(20–23). It is additionally a protein of great interest in cancer research because it is frequently mutated in a subset set of tumors(21). Given the interaction between CT224 and TRAF7, we renamed CT224 to TRAF7 Interactor 1 (Tri1).

In this work, we confirmed that the interaction between Tri1 and TRAF7 occurs during infection. In chapter 2, we defined the regions of Tri1 and TRAF7 that form the

binding interface and discovered that Tri1 can disrupt native TRAF7 protein-protein interactions. This work has been submitted for publication and is posted on BioRxiv(24). In Chapter 3, we describe our work that employs an orthogonal AP-MS-based approach in which we define the TRAF7 protein interactome and identify host proteins whose interactions with TRAF7 are decreased by displacement or increased by forming a new binding interface upon addition of Tri1. We further refine this data set by curating a set of TRAF7-host protein interactions that are present in the Tri1-host protein interactome and that are enhanced when Tri1 is added to TRAF7. Interestingly, a group of nuclear importer/exporter proteins was found in both data sets. We present preliminary evidence that one member, IPO5, is recruited to the inclusion in a Tri1-dependent manner. In Chapter 4, we performed host cell transcriptomics in cultured human cells infected with either wild type *C. trachomatis* or with a strain in which Tri1 is depleted by CRISPRi. Our analysis suggests that Tri1 may have a subtle effect on host cell signaling under the conditions of our infections.

This dissertation contributes to the further characterization of *C. trachomatis* Incs and aids in the understanding of how these effectors may modulate host cells. We additionally present the extensive role an Inc could play in altering protein-protein interactions through the binding of a single host protein, which may have consequences for cellular signaling. Additionally, we suggest that the Inc Tri1 is a potential tool to study the protein TRAF7 in the context of tumorigenesis. This work may thus further our understanding of the pathogenesis *C. trachomatis* infections, particularly how it remodels host cell signaling, and may provide further insights into the biological functions of the poorly understood host ubiquitin ligase TRAF7.

REFERENCES

1. Mogensen TH. 2009. Pathogen Recognition and Inflammatory Signaling in Innate Immune Defenses. *Clinical Microbiology Reviews* 22:240–273.
2. Hopfner K-P, Hornung V. 2020. Molecular mechanisms and cellular functions of cGAS–STING signalling. *Nat Rev Mol Cell Biol* 21:501–521.
3. Maculins T, Fiskin E, Bhogaraju S, Dikic I. 2016. Bacteria-host relationship: ubiquitin ligases as weapons of invasion. *Cell Res* 26:499–510.
4. Haldar AK, Saka HA, Piro AS, Dunn JD, Henry SC, Taylor GA, Frickel EM, Valdivia RH, Coers J. 2013. IRG and GBP Host Resistance Factors Target Aberrant, “Non-self” Vacuoles Characterized by the Missing of “Self” IRGM Proteins. *PLOS Pathogens* 9:e1003414.
5. Haldar AK, Piro AS, Finethy R, Espenschied ST, Brown HE, Giebel AM, Frickel E-M, Nelson DE, Coers J. 2016. *Chlamydia trachomatis* Is Resistant to Inclusion Ubiquitination and Associated Host Defense in Gamma Interferon-Primed Human Epithelial Cells. *mBio* 7.
6. Finethy R, Coers J. 2016. Sensing the enemy, containing the threat: cell-autonomous immunity to *Chlamydia trachomatis*. *FEMS Microbiol Rev* 40:875–893.
7. *Chlamydia*. <https://www.who.int/news-room/fact-sheets/detail/chlamydia>. Retrieved 19 March 2024.
8. Mohseni M, Sung S, Takov V. 2024. *Chlamydia* StatPearls. StatPearls Publishing, Treasure Island (FL).
9. Elwell C, Mirrashidi K, Engel J. 2016. *Chlamydia* cell biology and pathogenesis. *Nature Reviews Microbiology* 14:385–400.

10. Rucks EA. 2023. Type III Secretion in Chlamydia. *Microbiology and Molecular Biology Reviews* 87:e00034-23.
11. Rockey DD, Scidmore MA, Bannantine JP, Brown WJ. 2002. Proteins in the chlamydial inclusion membrane. *Microbes Infect* 4:333–40.
12. Bannantine JP, Griffiths RS, Viratyosin W, Brown WJ, Rockey DD. 2000. A secondary structure motif predictive of protein localization to the chlamydial inclusion membrane. *Cell Microbiol* 2:35–47.
13. Lutter EI, Martens C, Hackstadt T. 2012. Evolution and Conservation of Predicted Inclusion Membrane Proteins in Chlamydiae. *International Journal of Genomics* 2012:e362104.
14. Mirrashidi KM, Elwell CA, Verschueren E, Johnson JR, Frando A, Von Dollen J, Rosenberg O, Gulbahce N, Jang G, Johnson T, Jager S, Gopalakrishnan AM, Sherry J, Dunn JD, Olive A, Penn B, Shales M, Cox JS, Starnbach MN, Derre I, Valdivia R, Krogan NJ, Engel J. 2015. Global Mapping of the Inc-Human Interactome Reveals that Retromer Restricts Chlamydia Infection. *Cell Host Microbe* 18.
15. Elwell CA, Czudnochowski N, Dollen J, Johnson JR, Nakagawa R, Mirrashidi K, Krogan NJ, Engel JN, Rosenberg OS. 2017. Chlamydia interfere with an interaction between the mannose-6-phosphate receptor and sorting nexins to counteract host restriction. *Elife* 6.
16. Meier K, Jachmann LH, Türköz G, Babu Sait MR, Pérez L, Kepp O, Valdivia RH, Kroemer G, Sixt BS. 2023. The Chlamydia effector CpoS modulates the inclusion microenvironment and restricts the interferon response by acting on Rab35. *mBio* 14:e03190-22.

17. Mirrashidi KM, Elwell CA, Verschueren E, Johnson JR, Frando A, Von Dollen J, Rosenberg O, Gulbahce N, Jang G, Johnson T, Jäger S, Gopalakrishnan AM, Sherry J, Dunn JD, Olive A, Penn B, Shales M, Cox JS, Starnbach MN, Derre I, Valdivia R, Krogan NJ, Engel J. 2015. Global Mapping of the Inc-Human Interactome Reveals that Retromer Restricts Chlamydia Infection. *Cell Host & Microbe* 18:109–121.
18. Zotti T, Vito P, Stilo R. 2012. The seventh ring: Exploring TRAF7 functions. *Journal of Cellular Physiology* 227:1280–1284.
19. Dhillon B, Aleithan F, Abdul-Sater Z, Abdul-Sater AA. 2019. The Evolving Role of TRAFs in Mediating Inflammatory Responses. *Front Immunol* 10:104.
20. Zotti T, Vito P, Stilo R. 2012. The seventh ring: Exploring TRAF7 functions. *Journal of Cellular Physiology* 227:1280–1284.
21. Zotti T, Scudiero I, Vito P, Stilo R. 2017. The Emerging Role of TRAF7 in Tumor Development. *J Cell Physiol* 232:1233–1238.
22. Bouwmeester T, Bauch A, Ruffner H, Angrand PO, Bergamini G, Croughton K, Cruciat C, Eberhard D, Gagneur J, Ghidelli S, Hopf C, Huhse B, Mangano R, Michon AM, Schirle M, Schlegl J, Schwab M, Stein MA, Bauer A, Casari G, Drewes G, Gavin AC, Jackson DB, Joberty G, Neubauer G, Rick J, Kuster B, Superti-Furga G. 2004. A physical and functional map of the human TNF-alpha/NF-kappa B signal transduction pathway. *Nat Cell Biol* 6:97–105.
23. Xu LG, Li LY, Shu HB. 2004. TRAF7 potentiates MEKK3-induced AP1 and CHOP activation and induces apoptosis. *The Journal of biological chemistry* 279:17278–82.
24. Herrera CM, McMahon E, Swaney DL, Sherry J, Pha K, Adams-Boone K, Johnson JR, Krogan NJ, Stevers M, Solomon D, Elwell C, Engel J. 2024. The

Chlamydia trachomatis Inc Tri1 interacts with TRAF7 to displace native TRAF7 interacting partners. bioRxiv <https://doi.org/10.1101/2024.02.26.581999>.

CHAPTER 2 THE *CHLAMYDIA TRACHOMATIS* INC TRI1 INTERACTS WITH TRAF7
TO DISPLACE NATIVE TRAF7 INTERACTING PARTNERS

SUMMARY

Chlamydia trachomatis is the leading cause of bacterial sexually transmitted infections in the US and of preventable blindness worldwide. This obligate intracellular pathogen replicates within a membrane-bound inclusion, but how it acquires nutrients from the host while avoiding detection by the innate immune system is incompletely understood. *C. trachomatis* accomplishes this in part through the translocation of a unique set of effectors into the inclusion membrane, the inclusion membrane proteins (Incs). Incs are ideally positioned at the host-pathogen interface to reprogram host signaling by redirecting proteins or organelles to the inclusion. Using a combination of co-affinity purification, immunofluorescence confocal imaging, and proteomics, we characterize the interaction between an early-expressed Inc of unknown function, Tri1, and tumor necrosis factor receptor associated factor 7 (TRAF7). TRAF7 is a multi-domain protein with a RING finger ubiquitin ligase domain and a C-terminal WD40 domain. TRAF7 regulates several innate immune signaling pathways associated with *C. trachomatis* infection and is mutated in a subset of tumors. We demonstrate that Tri1 and TRAF7 specifically interact during infection and that TRAF7 is recruited to the inclusion. We further show that the predicted coiled-coil domain of Tri1 is necessary to interact with the TRAF7 WD40 domain. Finally, we demonstrate that Tri1 displaces the native TRAF7 binding partners, mitogen activated protein kinase kinase kinase 2 (MEKK2) and MEKK3. Together, our results suggest that by displacing TRAF7 native binding partners, Tri1 has the capacity to alter TRAF7 signaling during *C. trachomatis* infection.

INTRODUCTION

Chlamydia trachomatis is the most common cause of sexually transmitted bacterial infections and the leading cause of non-congenital blindness in developing nations(1). Complications associated with the sexually transmitted serovars include ectopic pregnancy, infertility, and pelvic inflammatory disease. Although effective antibiotic therapy exists, genital *C. trachomatis* infections are most commonly asymptomatic. Moreover, no therapy is cost-effective enough for use in developing nations, and an effective vaccine is still elusive(2). Elucidating the cellular and molecular mechanisms that contribute to *C. trachomatis* pathogenesis would allow the development of more targeted forms of treatment for the disease and could lead to the development of a vaccine.

Chlamydia species are obligate intracellular pathogens that share a common life cycle in which they alternate between the infectious extracellular elementary body (EB) and the intracellular replicative reticulate body (RB)(3). Upon binding to the host cell, EBs are internalized within a membrane-bound compartment through receptor-mediated endocytosis. *Chlamydia* avoids detection by the cytosolic innate immune response and escapes lysosomal degradation by modifying this compartment to create a unique intracellular replicative niche, the inclusion. *Chlamydia* species employ a specialized protein secretion apparatus, the type III secretion system, that translocates up to ~150 bacterial effectors into the host cytosol or into the inclusion membrane(4). This latter group, the inclusion membrane proteins (Incs), are unique to the order *Chlamydiales*(5). They are characterized by the presence of two or more closely-linked predicted transmembrane domains with their N- and C- termini exposed to the host cell cytosol(6,

7). The roles of most *Chlamydia* secreted effectors, including the Incs, remain incompletely described(8), as bioinformatics has been unrevealing and conventional genetic manipulation of *Chlamydia* species has only recently been achieved(9). Based on their topology and on functional studies, Incs may function as scaffolds to recruit and/or subvert host cell proteins or organelles(3, 10–12).

To test this hypothesis and to identify host interacting partners that would give insights into Inc function, we previously performed a high throughput affinity purification-mass spectrometry (AP-MS) screen using epitope-tagged *C. trachomatis* serovar D Incs transfected into human cells (hereafter referred to as the “transfection interactome”)(13). This screen identified potential binding partners for ~2/3 of the 58 predicted *C. trachomatis* serovar D Incs, including a predicted high confidence interaction between the ubiquitin ligase TRAF7 and CT224/CTL047 (hereafter renamed Tri1, for TRAF7 interactor). Here, we investigated the Tri1:TRAF7 interaction because Tri1 is not a well-characterized Inc and because TRAF7 is involved in signaling pathways that are relevant for *Chlamydia* infection. Thus, decoding the Tri1:TRAF7 interaction may provide insights into *C. trachomatis* pathogenesis.

Tri1 is expressed early and throughout infection(14) and localizes to the inclusion membrane(15). TRAF7 is part of the tumor necrosis receptor-associated factor (TRAF) family of proteins, which use a modular structure to mediate assembly of cytoplasmic signal transducers with regulator molecules downstream of receptor complexes(16). Each TRAF family member is thought to have distinct biological roles, even though TRAFs 1-6 regulate overlapping signaling pathways, including immune signaling(16, 17). Similarly to many of the other TRAFs, TRAF7 contains a coiled-coil domain important in

multimerization(18, 19), a zinc (Zn) finger domain, and RING finger ubiquitin ligase domain(18, 20, 21). However, unlike the other TRAFs, TRAF7 encodes a WD40 domain, a known protein scaffolding domain(22), in place of a canonical TRAF domain, at its C-terminus(21).

In this work, we show that Tri1 and TRAF7 specifically interact during infection and that TRAF7 is recruited to the inclusion. We further show that the predicted coiled-coil domain of Tri1 is necessary and likely sufficient to interact with the TRAF7 WD40 domain. Finally, we demonstrate that Tri1 displaces native TRAF7 binding partners, mitogen activated protein kinase kinase kinase 2 (MEKK2) and MEKK3. Together, our results suggest that Tri1 has the capacity to modulate TRAF7 protein-protein interactions and potentially to alter TRAF7 signaling during infection.

RESULTS

TRAF7 co-affinity purifies with Tri1.

Our previously published Inc-human transfection interactome predicted a high-confidence interaction between Tri1 (from *C. trachomatis* serovar D) transiently expressed in HEK293T cells and the human ubiquitin ligase TRAF7(13). Given that *C. trachomatis* genetics is most well developed for serovar LGV434/L2(9) and that Tri1 is highly conserved between serovars D and L2 (98% identity, Fig S2.1), we performed all subsequent studies with L2. We used two approaches to evaluate whether Tri1 interacts with TRAF7 in the context of L2 infection.

First, we performed affinity purifications (AP) from lysates of HeLa cells that were first transfected with mCherry (mCh)-TRAF7 for 24 hrs and then infected cells with L2 transformed with a plasmid expressing Tri1 (Tri1_{FLAG}) under the control of an anhydrous tetracycline (aTc)-inducible promoter (L2+pTri1_{FLAG}). As a control for Inc specificity, we infected cells in parallel with L2 transformed with a plasmid expressing IncG_{FLAG} (L2+pIncG_{FLAG}), an unrelated Inc. Immunoblot analysis of eluates demonstrated that TRAF7 co-affinity purifies (co-APs) with Tri1_{FLAG} but not with IncG_{FLAG} (Fig 2.1A).

Second, as the above experiment was performed with transfected TRAF7, we used AP-MS to determine whether endogenous TRAF7 co-APs with Tri1 during infection. Lysates from HeLa cells infected with L2+pTri1_{FLAG} in the presence of inducer were affinity purified using FLAG beads, and the eluates were analyzed by Liquid Chromatography (LC)/MS-MS. As controls for specificity, we performed LC/MS-MS on eluates prepared in parallel from cells infected with L2+pVector or from cells infected with L2 strains expressing Incs for which host binding partners are established, IncE(10, 13, 23, 24)

(L2+pIncE_{FLAG}) and Dre1(13, 25) (L2+pDre1_{FLAG}). Protein-protein interactions were scored by SAINT(26), which uses a scale of 0 to 1. The SAINT score of 1 for the Tri1_{FLAG}:TRAF7 interaction with a Bayesian False Discovery Rate (BFDR) of 0 indicates a high confidence and specific interaction. It compares favorably with the SAINT score from previously validated interactions of IncE_{FLAG} with SNX5(10, 13, 23, 24) and of Dre1_{FLAG} with DCTN4(13, 25). No spectral counts were detected for TRAF7 in the eluates analyzed from IncE_{FLAG} or Dre1_{FLAG} (Fig 2.1B), demonstrating the specificity of TRAF7 binding to Tri1. Likewise, no other TRAFs nor any other WD40-domain containing proteins were found to co-AP with Tri1. We thus conclude that in the context of transfection and infection, the interaction between Tri1 and TRAF7 is specific.

TRAF7 is recruited to the inclusion.

Having confirmed that Tri1 and TRAF7 interact during infection, we tested the prediction that Tri1 would recruit TRAF7 to the inclusion. We confirmed that Tri1_{FLAG} localized to the inclusion membrane (Fig 2.2), consistent with published results of others(15). We next examined the localization of mCh-TRAF7 and endogenous TRAF7 in cells infected with L2+pTri1_{FLAG}. We observed that mCh-TRAF7 was robustly recruited to the inclusion in the presence of inducer (Fig 2.2A). We observed occasional recruitment of mCh-TRAF7 to the inclusions in infections performed in the absence of inducer (Fig 2.2A), likely due to chromosomally expressed Tri1.

To examine the recruitment of endogenous TRAF7, we first validated a commercially available antibody to TRAF7 by immunofluorescence and by immunoblot analysis (Fig S2.2). Both endogenous TRAF7 and FLAG-TRAF7 could be detected by

immunoblot (Fig S2.2A). We observed that endogenous TRAF7 and mCh-TRAF7 localized to the nucleus, cytosol, and cytoplasmic puncta (Fig S2.2B, C), consistent with previously published results(18, 27, 28).The cytoplasmic puncta were particularly prominent upon transfection, suggesting that TRAF7 puncta formation is enhanced when the protein is overexpressed, as has been reported for all of the TRAFs(29). In HeLa cells infected with L2+pTri1_{FLAG} for 24 hrs, we observed recruitment of endogenous TRAF7 to the inclusion in the presence of inducer (Fig 2.2B). Although recruitment of endogenous TRAF7 appears to be enhanced when Tri1 is overexpressed, it was not possible to quantify due to the low levels of detection of endogenous TRAF7 by the antibody.

The predicted coiled-coil domain of Tri1 interacts with the WD40 domain of TRAF7

We next defined the regions of Tri1 and TRAF7 that are necessary and sufficient for their interaction by co-transfection followed by co-AP studies using deletion mutants (Figs 2.3 and 2.4). Tri1 has a canonical Inc structure(15), with two closely linked transmembrane domains, a short N-terminal domain predicted to encode the type three secretion signal, and a C-terminal domain(Fig 2.3A). Although alpha-fold analysis(30) predicts that the C-terminus would assume an alpha-helical structure, multiple coiled-coil prediction algorithms(31) suggest that the C-terminus encodes a coiled-coil domain. Based on these analyses, we assigned residues 118 to 138 for the coiled-coil domain of Tri1.

To determine if the coiled-coiled domain was necessary for Tri1 binding to TRAF7, we co-transfected HEK293T cells with full-length FLAG-TRAF7 and with Strep-tagged constructs of Tri1 that either completely lack the coiled-coil domain (Tri1₁₋₁₁₇, Fig 3A) or

that have a truncated coiled-coil domain (Tri1₁₋₁₂₈, Fig 2.3A). To determine if the coiled-coil domain was sufficient for Tri1 binding to TRAF7, we fused Tri1₈₄₋₁₄₇ to superfolder GFP (sfGFP), in addition to Strep (Fig 2.3A), to enhance its stability. Tri1-Strep or Tri1-sfGFP-Strep served as full-length controls. Lysates were affinity purified on Strep-Tactin beads. TRAF7 co-AP'd only with Tri1 variants containing the complete predicted coil-coil domain (Tri1 and Tri1₈₄₋₁₄₇; Fig 2.3B), indicating that the coiled-coil domain is necessary and likely sufficient for the Tri1:TRAF7 interaction.

TRAF7 encodes several annotated domains(18, 20, 21), including an N-terminal RING finger ubiquitin ligase domain, a zinc (Zn) finger domain, a coiled-coil domain, and seven WD40 repeats that form the WD40 domain (Fig 2.4A). We predicted that the interaction between TRAF7 and Tri1 is likely mediated by the WD40 domain, as only TRAF7, among the TRAF family members, encodes a WD40 domain(16), and no other proteins containing a WD40 domain were found to co-AP with Tri1. To test this hypothesis, we performed co-APs on lysates prepared from HEK293T cells transfected with Tri1-Strep and with TRAF7 variants. Only TRAF7 variants containing the WD40 domain (TRAF7, TRAF7_{CC+WD40}, and TRAF7_{WD40}) co-AP'd with Tri1 (Fig. 2.4B). We thus conclude that the TRAF7 WD40 domain is necessary and sufficient for binding to Tri1.

We additionally tested whether the WD40 domain of TRAF7 was necessary or sufficient for its recruitment to the inclusion. We observed that mCh-TRAF7_{WD40} and full-length mCh-TRAF7 were recruited to the inclusions of cells infected with L2+pTri1_{FLAG} in the presence of inducer. In contrast, the TRAF7 variant that lacks the WD40 domain (mCh-TRAF7_{ΔWD40}) exhibited minimal recruitment (Fig 2.4C). We speculate that this

residual recruitment to the inclusion is likely due to the ability of mCh-TRAF7 $_{\Delta$ WD40 to multimerize with endogenous TRAF7 (18, 19).

Tri1 displaces native TRAF7 interacting partners MEKK2 and MEKK3.

We considered whether binding of Tri1 to TRAF7 $_{\text{WD40}}$ domain could disrupt native TRAF7 protein-protein interactions. For this purpose, we employed an unbiased quantitative AP-MS approach to identify native binding partners of the WD40 domain of TRAF7 whose interactions are disrupted in the presence of the coiled-coil domain of Tri1 but not by a Tri1 variant that lacks this domain (Fig 2.5A). Cells co-transfected with empty-FLAG vector and Tri1-Strep served as negative controls. SAINT analysis identified MEKK2 as a significant interactor of TRAF7 $_{\text{WD40}}$ in the presence of the truncated Tri1 (Tri1 $_{1-128}$), with a SAINT score of 1 and a BFDR of 0 (Fig 2.5B). However, in a parallel experiment in which full length Tri1 was co-transfected with TRAF7 $_{\text{WD40}}$, no spectral counts for MEKK2 were identified by AP-MS (Fig 2.5B). This analysis suggests that MEKK2 is a native interactor of the WD40 domain of TRAF7. Furthermore, our results demonstrate that Tri1 displaces MEKK2 from TRAF7 in a manner dependent upon the complete coil-coil domain of Tri1. We identified other interactors of the TRAF7 WD40 domain, including T-complex protein 1 subunit subunits delta and gamma (TCPD, TCPG) and DnaJ homolog subfamily A member 2 (DNJA2), which bound to TRAF7 in the presence of either Tri1 or Tri1 $_{1-128}$ (Fig 5B), indicating the Tri1-mediated displacement of MEKK2 is specific.

MEKK3, a closely related homolog of MEKK2, has also been reported to interact with the WD40 domain of TRAF7(18, 20). However, we did not detect MEKK3 in our AP-

MS data set for unclear reasons. We therefore tested whether Tri1 can disrupt MEKK2 or MEKK3 binding from the TRAF7 WD40 domain by co-transfection studies. HEK293T cells were co-transfected with Tri1-Strep or Tri1₁₋₁₂₈-Strep and either FLAG-TRAF7_{WD40} (Figs 2.5C, E) or FLAG-TRAF7 (Fig 2.5D). For the MEKK3 displacement experiments, we additionally co-transfected cells with Myc-MEKK3 (Fig 2.5E). Lysates were affinity purified over FLAG beads and eluates were analyzed by immunoblot. Tri1, but not the non-binding variant (Tri1₁₋₁₂₈) decreased the binding of MEKK2 to both TRAF7_{WD40} (Fig 2.5C) and to TRAF7 (Fig 2.5D). Similarly, Tri1, but not the non-binding variant (Tri1₁₋₁₂₈), decreased the binding of myc-MEKK3 to TRAF7_{WD40} (Fig 2.5E). Together, our studies demonstrate that Tri1, through its coiled-coil domain, can displace the TRAF7 native binding partners MEKK2 and MEKK3.

DISCUSSION

As a successful intracellular pathogen, *Chlamydia* must replicate intracellularly while avoiding immune detection(3, 12, 32). Although *C. trachomatis* induces cell-autonomous signaling pathways, including the cGAS-STING, NF- κ B, and JNK-AP-1 pathways, it must modulate their downstream effects to survive intracellularly(3, 12, 33). *C. trachomatis* is thought to regulate some of these pathways through the secretion of soluble effectors, including Incs(3, 11, 12). For example, upon transfection, the secreted effector Cdu1, a deubiquitinase and acetyltransferase(34), can inhibit NF- κ B signaling(35). Additionally, the Inc CpoS can inhibit STING activation, possibly through its interaction with a subset of Rab GTPases(36, 37). However, no *C. trachomatis* Incs have as yet been linked to JNK-AP1 signaling, a pathway which is induced late during infection and is important for its intracellular replication(33). Thus, further study into *C. trachomatis* effectors may elucidate how this intracellular bacterium can subvert major host signaling pathways.

Here, building on our previous work in which we defined the Inc-host interactome(13), we investigate the predicted interaction between Tri1 and TRAF7. We were particularly interested in this interaction because TRAF7 modulates key components of the innate immune response, including Type I interferon (IFN)(38, 39), NF- κ B, and JNK-AP-1 signaling(16). We demonstrate that Tri1 interacts with TRAF7 during infection and that it can recruit endogenous or transfected TRAF7 to the inclusion. We localized the Tri1:TRAF7 binding interface to the coiled-coil domain of Tri1 and the WD40 domain of TRAF7. Using AP-MS, we identified MEKK2 as a native TRAF7 interactor. Finally, through co-transfection studies, we confirmed that Tri1 binding to the WD40 domain of TRAF7

can displace MEKK2 as well as a closely related previously identified TRAF7 interactor, MEKK3(18, 20). While our experiments were in progress, others reported an interaction between TRAF7 and MEKK2, along with MEKK3 and with MEK5(40). Together, these experiments underscore that the TRAF7 WD40 domain can interact with a subset of constituents of the MAP kinase pathways.

By binding to host proteins, Incs have the potential to disrupt native host-protein interactions and/or to synergize with host binding partners to create new protein binding surfaces(3, 10–12). In our studies, we used an unbiased AP-MS-based strategy to define native binding partners of a host protein of interest that can be targeted by a microbial effector. This approach allowed us to identify a new TRAF7 interactor that could be displaced by an Inc. A major advantage of this approach is that it allows for the identification of host protein binding partners that can be displaced by an effector without knowing the specific residues required for the effector:host protein interaction. Moreover, this approach is equally applicable if the binding of an effector to a host target creates a new binding interface that recruits additional host proteins. Finally, the approach is easily scalable and widely applicable to any microbial effector, as demonstrated by our initial AP-MS screen to define the Inc-host interactome(13).

A major conundrum of TRAF7 biology is its roles in a wide array of signaling pathways, sometimes with reportedly contradictory outcomes. For example, TRAF7 has been shown to both promote or inhibit inflammation(16) by either activating(18, 20) or inhibiting(28) the NF- κ B signaling pathway. Additionally, TRAF7-dependent ubiquitination can inhibit type I IFN signaling(38, 39) and promote epithelial-mesenchymal transition (EMT)(41), a reprogramming event that is induced by *C. trachomatis* infection(42). Thus,

further study of the consequences of the Tri1:TRAF7 interaction may provide new insights into TRAF7 modulation of these important signaling pathways.

The WD40 domain of TRAF7 has recently emerged as a common mutational hot spot for a subset of unusual human tumors, including mesotheliomas(43, 44), adenomatoid tumors of the genital tract(45), fibromyxoid spindle cell sarcomas of soft tissue(46), perineurioma nerve sheath tumors(47), and meningiomas(48–50). Some of the mutations lead to increased NF- κ B signaling(45) and decreased JNK signaling. Particularly relevant to our studies of the Tri1:TRAF7 interaction are mutations within the TRAF7 WD40 domain associated with meningiomas. Transfection of these mutated proteins lead to decreased binding of MEKK3 to TRAF7 and decreased JNK signaling(40). These mutations predict potential residues that mediate the TRAF7:Tri1 interaction. Experiments to test this idea are underway.

Although data regarding the consequences of the TRAF7:MEKK2 interaction is limited, the role of TRAF7 in MEKK3 signaling is more well characterized(18, 20, 40). Therefore, we can speculate on how Tri1 displacement of MEKK3 from TRAF7 could modify host cell signaling. MEKK3 is a key signaling molecule in the TNF-induced NF- κ B activation pathway(51). TRAF7 can stimulate MEKK3 kinase activity(20), and MEKK3 can promote TRAF7 ubiquitin ligase activity(18). Together, the two proteins act synergistically, and possibly in the same complex, to stimulate the NF- κ B and JNK signaling pathways(18, 20). Additionally, TRAF7 is important for activating the MEKK3-MEK-ERK5 signaling pathway, which is involved in maintaining vascular cell integrity in response to fluid shear stress(40). This pathway has major consequences for cells, including inhibiting apoptosis, inflammation, and epithelial to mesenchymal transition(52), all of which could

be relevant to *C. trachomatis* infection(42). We predict that Tri1 displacement of MEKK2/3 from TRAF7 during *C. trachomatis* infection would lead to a downregulation of TRAF7 ubiquitin ligase activity and thus alter TRAF7-dependent signaling, such as NF- κ B, JNK, and MEKK3-MEK-ERK signaling(40).

Our identification of Tri1 as a TRAF7 interactor provides an excellent opportunity to tease apart the mechanistic functions of this important host protein in numerous signaling pathway related to developmental biology, immunology, and cancer biology. In this work, we focused on the TRAF7:MEKK2/3 complexes, but there are other TRAF7 protein-protein interactions which may be altered by Tri1 during infection. Thus, further investigation may identify additional native TRAF7 binding partners that are displaced by Tri1. Finally, it will be interesting to determine whether TRAF7 ubiquitin ligase activity and its related pathways are altered in a Tri1-dependent manner during infection. Examining these interactions will be key to fully understanding the role of Tri1 binding and recruitment of TRAF7 in *C. trachomatis* intracellular survival.

MATERIALS AND METHODS

Cell Culture and Bacterial Propagation

HeLa 229 and Vero cells were obtained from American Type Culture Collection (ATCC). HEK293T cells were a generous gift from Dr. Nevan Krogan (UCSF). TRAF7 isoform 1 CRISPR/Cas9 KO HeLa cells (Isoform 2 of TRAF7, which lacks residues 1-76 was not targeted by CRISPR/Cas9 and was thus still expressed in cells) were obtained from Abcam (ab264998, discontinued).

HeLa cells were cultured and maintained in Eagle's Minimum Essential Medium (MEM; UCSF Cell Culture Facility) supplemented with 10% (v/v) fetal bovine serum (FBS) from Gemini at 37°C in 5% CO₂. HEK293T and Vero cells were cultured and maintained in Dulbecco's modified Eagle's Medium (DMEM, UCSF Cell Culture Facility) supplemented with 10% (v/v) FBS at 37°C in 5% CO₂. Cells were routinely tested for mycoplasma (Molecular Probes, M-7006). *C. trachomatis* was routinely propagated in Vero cell monolayers as previously described(53). HeLa cells were used for all infection studies. HeLa and HEK293T cells were used for ectopic expression experiments. Stellar chemically competent *Escherichia coli* (Takara Bio) was used to prepare plasmids for ectopic expression in mammalian cells.

Antibodies and Reagents

Primary antibodies were obtained from the following sources: rabbit anti-RFP (Rockland, 600-401-379-RTU), mouse anti-FLAG (Millipore, F3165), rabbit anti-FLAG (Millipore, F7425), mouse anti-GAPDH (Millipore, MAB374), goat anti-MOMP L2 (Fitzgerald, 20C-CR2104GP), rabbit anti-TRAF7 (Novus Biologicals, NBP2-93316),

rabbit anti-Strep TagII HRP (Novagen, 71591–3), rabbit anti-MEKK2 (Abcam, ab33918), mouse anti-Myc (Thermo Fisher, R950-25). Mouse anti-IncA was kindly provided by Dr. Dan Rockey (Oregon State University). Secondary antibodies for immunofluorescence microscopy were derived from donkey and purchased from Life Technologies or Abcam: anti-rabbit Alexafluor 568, anti-rabbit Alexafluor 488, anti-mouse Alexafluor 405, anti-goat Alexafluor 647.

A plasmid expressing Tri1₈₄₋₁₄₇-GFP (serovar D) was a generous gift from Dr. Raphael Valdivia (Duke University). Myc-MEKK3 (K391A, pcDNA3.1) was originally provided by Dr. Xin Lin (Addgene plasmid # 44157; <http://n2t.net/addgene:44157>; RRID:Addgene_44157). *C. trachomatis* L2 (434/Bu) was a generous gift from Deborah Dean (UCSF). The *C. trachomatis* L2 strains overexpressing Tri1_{FLAG} (originally “CT224-FLAG”) and Dre1_{FLAG} were generous gifts from Drs. Mary Weber (University of Iowa) and Ted Hackstadt (Rocky Mountain Laboratories). The *C. trachomatis* L2 strain overexpressing IncE_{FLAG} and IncG_{FLAG} were generous gifts from Dr. Isabelle Derré (University of Virginia). Primers (Table S1) were commercially generated by Integrated DNA Technologies or by Elim Biopharm.

Plasmid Construction

The Tri1-Strep constructs used for ectopic expression studies were PCR amplified from genomic *C. trachomatis* L2 (434/Bu) DNA and subcloned into the EcoRI and NotI sites in pcDNA4.0/2xStrepII(54) using In-Fusion cloning (Takara) Tri1-Strep-sfGFP was generated by subcloning superfolder (sf) GFP (from Dre1-sfGFP) into Tri1-Strep

constructs (Full length or Tri1₈₄₋₁₄₇) at the Xho1 and Apa1 sites as a C-terminal fusion(25). TRAF7 constructs were amplified from pUC57-TRAF7 (a plasmid expressing full-length TRAF7) and subcloned into the HindIII and KpnI sites in pmCherry C1 and pcDNA4.0/3X FLAG vector using In-Fusion cloning. All TRAF7 constructs are tagged at the N-terminus and all Tri1 constructs are tagged at the C-terminus. Wild-type Myc-MEKK3 (in pcDNA3.1 vector) was generated from a kinase-dead mutant (K391A, Addgene plasmid # 44157)(55) using QuikChange Lightning Site-Directed Mutagenesis (Agilent). Only wild-type Myc-MEKK3 was used for experiments. Constructs were verified by forward and reverse sequencing.

Affinity Purifications

For Strep-Tactin affinity purifications in the context of transfections, HEK293T (6 x 10⁶ cells per plate) were seeded in one to three 10 cm² plates. For FLAG affinity purifications, HeLa cells (3 x 10⁵ cells) were seeded in each well of two 6-well plates. Cells were transfected with the indicated constructs using Continuum Transfection Reagent (GeminiBio), following manufacturer's instructions. At 48 hrs post-transfection, cells were scraped on ice, pelleted, washed with PBS, and lysed in 1 mL cold Wash Buffer (50 mM Tris HCL pH 7.5, 150 mM NaCl, 1 mM EDTA) plus 0.5% IGEPAL (Sigma), Complete protease (Roche) and PhosSTOP phosphatase inhibitor (Roche). Lysates were added to 60 µL of FLAG beads (Sigma) or 60 µL of Strep-Tactin Sepharose beads (IBA) and incubated with rotation overnight at 4° C. Beads were washed three times in Wash Buffer plus 0.05% IGEPAL, and finally once in Wash Buffer without detergent. Samples were eluted in 45 µL of FLAG peptide (300 µg/mL, Millipore Sigma) in Wash Buffer plus

0.05% RapiGest (Waters Corp) for FLAG APs or in 45 μ L of 10 mM D-desthiobiotin (IBA) in Final Wash Buffer for Strep APs.

For FLAG APs in the context of L2 infections, HeLa cells were grown to 70% confluency (0.84×10^6 cells/well) in three 6-well plates per condition. Cells were transfected (as described above) with mCh-TRAF7 for 24 hrs prior to infection with L2+pTri1_{FLAG} or L2+ pIncG_{FLAG} at a multiplicity of infection (MOI) of 5. L2 strains were suspended in MEM supplemented with 10% FBS, centrifuged at 1000 RPM for 30 min at room temperature onto HeLa cells grown on coverslips. Infected cells were incubated at 37°C in 5% CO₂ for 1 hr. Infection media was aspirated off, fresh media containing no aTc or 200 ng/mL aTc was added, and cells were incubated at 37°C in 5% CO₂ for 24 hrs. Cells were treated with 10 μ M MG132 (Cayman Chemicals) 4 hours prior to lysis and processed for FLAG APs as described above.

For co-APs for MS to determine the interactome of TRAF7, HEK293T were seeded at a density of 6×10^6 cells per 10 cm plate for next day transfection. Two plates were used per transfection condition. Cells were transfected with FLAG-TRAF7_{WD40} and Tri1-Strep using Continuum transfection reagent (Gemini Bio) or Effectene transfection reagent (Qiagen). For control conditions, cells were transfected with empty FLAG-vector and Tri1-Strep (full length or Tri1₁₋₁₂₈-Strep). At 44 hrs post-transfection, cells were treated with 10 μ M MG132. At 48 hrs post-transfection, cells were scraped on ice, pelleted, washed with PBS, and lysed in 1 mL cold Wash Buffer and subjected to FLAG APs as described above.

To determine the interactome of Tri1_{FLAG}, eight 6-well plates of 80% confluent HeLa cells were infected with either *C. trachomatis* L2 expressing plasmid-encoded Incs

(L2+pTri1_{FLAG}, L2+ plncE_{FLAG}, or L2+pDre1_{FLAG}) or empty vector at an MOI of 5 for 36 hrs as previously described (25). 10 μ M MG132 was added 4 hours prior to lysis, and cells were lysed on the plates for 30 min at 4 C in Lysis Buffer (50 mM Tris-HCl pH 7.5, 150 mM NaCl, 1 mM EDTA, 0.5% NP-40, PhosStop, Roche Complete Protease Inhibitor). Lysates were clarified by centrifugation at 13,000 RPM, 4.C for 15 min. Supernatants were then incubated with 30 μ l anti-FLAG magnetic beads (Millipore Sigma) rotating overnight at 4°C. Beads were washed three times in Wash Buffer (50 mM Tris-HCl pH 7.5, 150 mM NaCl, 1 mM EDTA, 0.05% NP-40) and then once in Final Wash Buffer (50 mM Tris-HCl pH 7.5, 150 mM NaCl, 1 mM EDTA). Samples were eluted in 45 μ l of Elution Buffer (100 μ g/mL FLAG peptide in Final Wash Buffer; Millipore Sigma) for 25 min at room temperature with continuous gentle agitation. All AP-MS experiments were performed in triplicate and assessed by Immunoblotting with FLAG antibody using enhanced chemiluminescence (Amersham Biosciences) and by silver stain (Pierce).

MS sample preparation.

A solution of 10 μ L of 8 M urea, 250 mM Tris, 5 mM DTT was added to the eluate to achieve a final concentration ~1.7 M urea, 50 mM Tris, and 1 mM DTT. Samples were incubated at 60C for 15 min and allowed to cool to room temperature. Iodoacetamide was added to a final concentration of 3 mM and incubated at room temperature for 45 min in the dark. DTT was then added to a final concentration of 3 mM before adding 1 μ g of sequencing-grade trypsin (Promega) and incubating at 37C overnight. Digested peptide samples were acidified to 0.5% TFA (ph<2) with 10% TFA stock and desalted using C18 ultra micro spin columns (The Nest Group).

MS data acquisition and analysis.

For AP-MS experiments, samples were resuspended in 15 μ L of MS loading buffer (4% formic acid, 2% acetonitrile) and 2 μ L were separated by a reversed-phase gradient over a nanoflow 75 μ m ID x 25cm long picotip column packed with 1.9 μ M C18 particles (Dr. Maisch). Peptides were directly injected over the course of a 75 min acquisition into a Q-Exactive Plus mass spectrometer (Thermo) and data was acquired in a data-dependent acquisition mode. Raw MS data were searched against the uniprot canonical isoforms of the human proteome (downloaded February 28, 2020) and the *C. trachomatis* L2 Strain434BuATCCVR-902B proteome, using the default settings in MaxQuant (version 1.6.12.0), with a 0.7min match-between-runs time window enabled(56). Peptides and proteins were filtered to 1% false discovery rate in MaxQuant, and identified proteins were then subjected to protein-protein interaction scoring. For protein-protein interaction (PPI) scoring, protein spectral counts as determined by MaxQuant search results were used for PPI confidence scoring by SAINTexpress (version 3.6.1)(26). For the TRAF7_{WD40} data analysis cells, co-transfected with empty FLAG vector and either Tri1-Strep or Tri1₁₋₁₂₈-Strep were used as negative controls. For the infection data analysis, HeLa cells infected with L2 transformed with a plasmid expressing an empty FLAG vector was used as a negative control. SAINT analysis was conducted on data from 9 L2 strains each expressing a different FLAG-tagged Inc.

Fluorescence microscopy

HeLa cells were seeded (1.2×10^6 cells/well, 3 wells per condition) and grown on acid-treated glass coverslips (Warner Instruments) in 24-well plates. Cells were transfected using Effectene as described above.

For fluorescence microscopy of L2-infected HeLa cells, L2 strains were suspended in MEM supplemented with 10% FBS, centrifuged at 1000 RPM for 30 min at room temperature onto HeLa cells grown on coverslips. Infections were performed at an MOI of 1. Infected cells were incubated at 37°C in 5% CO₂ for 1 hr. Infection media was aspirated off, fresh media containing no aTc or 50 ng/mL aTc was added, and cells were incubated at 37°C in 5% CO₂ for 24 or 48 hrs.

Cells were fixed in 4% PFA in PBS for 15 min at room temperature and then permeabilized in 0.2% Triton X-100 in PBS for 15 min at room temperature. Cells were blocked in PBS containing 1% BSA for 1 hr and then stained with the appropriate primary antibody (overnight) and secondary antibody (1 hr) in 1% BSA. Coverslips were mounted on Vectashield mounting media with or without DAPI (Vector Laboratories).

Images were acquired using Yokogawa CSU-X1 spinning disk confocal mounted on a Nikon Eclipse Ti inverted microscope equipped with an Andora Clara digital camera and CFI APO TIRF 60X oil or PLAN APO 40x objective. Single Z slices were acquired for all images shown. Images were acquired by NIS-Elements software 4.10 (Nikon). For each set of experiments, the exposure time for each filter set for all images was identical. Images were processed using FIJI Software.

Bioinformatics

The coiled-coil domain of Tri1 from was predicted by submitting the full-length protein sequence for Tri1 from *C. trachomatis* L2 (434/Bu) to waggawagga, which includes Multicoil and NCOILS predictions(31). Additionally, the Tri1 coiled-coil domain was previously annotated on Uniprot by COILS(57) (Uniprot ID: A0A0H3MBY0, <https://rest.uniprot.org/unisave/A0A0H3MBY0?format=txt&versions=12>) as residues 118 to 138. This coiled-coil domain prediction was used for Tri1 mutant construction. Transmembrane domain predictions were conducted using Phobius(58).

Data Availability

All AP-MS raw data files and search results are available from the Pride partner ProteomeXchange repository under the PXD049432 identifier(59, 60).They can be accessed with the following login credentials: Username: reviewer_pxd049432@ebi.ac.uk Password: aa8xT6vP.

ACKNOWLEDGEMENTS

We thank Raphael Valdivia (Duke University), Deborah Dean (UCSF), Mary Weber (University of Iowa), Ted Hackstadt (Rocky Mountain Laboratories), Xin Lin (University of Texas, M.D. Anderson Cancer Center), Dan Rockey (Oregon State University), and Isabelle Derre (University of Virginia) for reagents. J.E., C.H., E.M., K.A-B., J.S., K.P., D.S., J.R., N.K. C.E., were supported by funding provided by the NIH (R56 AI152526, RO1 AI122747). C.H. was also supported by NIH F31 AI52286, T32 AI 60537, T32 GM007810, and the UCSF Discovery Fellows program. J.S. was also supported by NIH F31 AI133951. K.P. was also supported NIH F32 AI133902.

Author contributions

Conceptualization, C.H., E.M., J.S., K.P., C.E., J.E.; Data curation, D.S.; Formal analysis, J.J., D.S.; Funding acquisition, C.H., J.E.; Investigation, C.H., E.M., K. A-B., C.E., J.E.; Methodology, C.H., E.M., D.S., J.S., K.P., C.E., J.E.; Project administration, D.S., N.K., C.E., J.E.; Resources, J.J., D.S., M.S.; Supervision, D.S., N.K., C.E., J.E.; Validation, C.H., E.M., D.S., C.E., J.E.; Visualization, C.H., J.S., K.P., C.E., J.E.; Writing—original draft, C.H., D.S., J.S., K.P., C.E., J.E.; Writing-revisions and editing, C.H., D.S., J.S., K.P., D.S., C.E., J.E.

Declaration of interests

The Krogan Laboratory has received research support from Vir Biotechnology, F. Hoffmann-La Roche, and Rezo Therapeutics. Nevan Krogan has a financially compensated consulting agreement with Maze Therapeutics. He is the President and is on the Board of Directors of Rezo Therapeutics, and he is a shareholder in Tenaya Therapeutics, Maze Therapeutics, Rezo Therapeutics, GEn1E Lifesciences, and Interline Therapeutics.

REFERENCES

1. Mohseni M, Sung S, Takov V. 2024. ChlamydiaStatPearls. StatPearls Publishing, Treasure Island (FL).
2. de la Maza LM, Zhong G, Brunham RC. 2017. Update on Chlamydia trachomatis Vaccinology. *Clinical and Vaccine Immunology* 24:e00543-16.
3. Elwell C, Mirrashidi K, Engel J. 2016. Chlamydia cell biology and pathogenesis. *Nat Rev Microbiol* 14:385–400.
4. Rucks EA. 2023. Type III Secretion in Chlamydia. *Microbiology and Molecular Biology Reviews* 87:e00034-23.
5. Lutter EI, Martens C, Hackstadt T. 2012. Evolution and Conservation of Predicted Inclusion Membrane Proteins in Chlamydiae. *International Journal of Genomics* 2012:e362104.
6. Bannantine JP, Griffiths RS, Viratyosin W, Brown WJ, Rockey DD. 2000. A secondary structure motif predictive of protein localization to the chlamydial inclusion membrane. *Cell Microbiol* 2:35–47.
7. Rockey DD, Scidmore MA, Bannantine JP, Brown WJ. 2002. Proteins in the chlamydial inclusion membrane. *Microbes Infect* 4:333–40.
8. Moore ER, Ouellette SP. 2014. Reconceptualizing the chlamydial inclusion as a pathogen-specified parasitic organelle: an expanded role for Inc proteins. *Frontiers in cellular and infection microbiology* 4:157.
9. Banerjee A, Nelson DE. 2021. The growing repertoire of genetic tools for dissecting chlamydial pathogenesis. *Pathog Dis* 79:ftab025.

10. Elwell CA, Czudnochowski N, von Dollen J, Johnson JR, Nakagawa R, Mirrashidi K, Krogan NJ, Engel JN, Rosenberg OS. 2017. Chlamydia interfere with an interaction between the mannose-6-phosphate receptor and sorting nexins to counteract host restriction. *Elife* 6.
11. Bugalhão JN, Mota LJ. The multiple functions of the numerous Chlamydia trachomatis secreted proteins: the tip of the iceberg. *Microb Cell* 6:414–449.
12. Stelzner K, Vollmuth N, Rudel T. 2023. Intracellular lifestyle of Chlamydia trachomatis and host–pathogen interactions. *Nat Rev Microbiol* 1–15.
13. Mirrashidi KM, Elwell CA, Verschueren E, Johnson JR, Frando A, Von Dollen J, Rosenberg O, Gulbahce N, Jang G, Johnson T, Jager S, Gopalakrishnan AM, Sherry J, Dunn JD, Olive A, Penn B, Shales M, Cox JS, Starnbach MN, Derre I, Valdivia R, Krogan NJ, Engel J. 2015. Global Mapping of the Inc-Human Interactome Reveals that Retromer Restricts Chlamydia Infection. *Cell Host Microbe* 18.
14. Shaw EI, Dooley CA, Fischer ER, Scidmore MA, Fields KA, Hackstadt T. 2000. Three temporal classes of gene expression during the Chlamydia trachomatis developmental cycle. *Molecular Microbiology* 37:913–925.
15. Weber MM, Bauler LD, Lam J, Hackstadt T. 2015. Expression and Localization of Predicted Inclusion Membrane Proteins in Chlamydia trachomatis. *Infection and Immunity* 83:4710–4718.
16. Zotti T, Vito P, Stilo R. 2012. The seventh ring: Exploring TRAF7 functions. *Journal of Cellular Physiology* 227:1280–1284.
17. Dhillon B, Aleithan F, Abdul-Sater Z, Abdul-Sater AA. 2019. The Evolving Role of TRAFs in Mediating Inflammatory Responses. *Front Immunol* 10:104.

18. Bouwmeester T, Bauch A, Ruffner H, Angrand PO, Bergamini G, Croughton K, Cruciat C, Eberhard D, Gagneur J, Ghidelli S, Hopf C, Huhse B, Mangano R, Michon AM, Schirle M, Schlegl J, Schwab M, Stein MA, Bauer A, Casari G, Drewes G, Gavin AC, Jackson DB, Joberty G, Neubauer G, Rick J, Kuster B, Superti-Furga G. 2004. A physical and functional map of the human TNF-alpha/NF-kappa B signal transduction pathway. *Nat Cell Biol* 6:97–105.
19. Song X, Hu R, Chen Y, Xiao M, Zhang H, Wu S, Lu Q. 2024. The structure of TRAF7 coiled-coil trimer provides insight into its function in zebrafish embryonic development. *Journal of Molecular Cell Biology* mjad083.
20. Xu L-G, Li L-Y, Shu H-B. 2004. TRAF7 Potentiates MEKK3-induced AP1 and CHOP Activation and Induces Apoptosis. *J Biol Chem* 279:17278–17282.
21. Zotti T, Scudiero I, Vito P, Stilo R. 2017. The Emerging Role of TRAF7 in Tumor Development. *J Cell Physiol* 232:1233–1238.
22. Stirnimann CU, Petsalaki E, Russell RB, Müller CW. 2010. WD40 proteins propel cellular networks. *Trends in Biochemical Sciences* 35:565–574.
23. Sun Q, Yong X, Sun X, Yang F, Dai Z, Gong Y, Zhou L, Zhang X, Niu D, Dai L, Liu J-J, Jia D. 2017. Structural and functional insights into sorting nexin 5/6 interaction with bacterial effector IncE. *Signal Transduct Target Ther* 2:17030.
24. Paul B, Kim HS, Kerr MC, Huston WM, Teasdale RD, Collins BM. 2017. Structural basis for the hijacking of endosomal sorting nexin proteins by *Chlamydia trachomatis*. *eLife* 6:e22311.
25. Sherry J, Dolat L, McMahon E, Swaney DL, Bastidas RJ, Johnson JR, Valdivia RH, Krogan NJ, Elwell CA, Engel JN. 2022. *Chlamydia trachomatis* effector Dre1

interacts with dynactin to reposition host organelles during infection. bioRxiv

<https://doi.org/10.1101/2022.04.15.488217>.

26. Teo G, Liu G, Zhang J, Nesvizhskii AI, Gingras AC, Choi H. 2014. SAINTexpress: improvements and additional features in Significance Analysis of INTERactome software. *J Proteomics* 100:37–43.

27. Morita Y, Kanei-Ishii C, Nomura T, Ishii S. 2005. TRAF7 Sequesters c-Myb to the Cytoplasm by Stimulating Its Sumoylation. *MBoC* 16:5433–5444.

28. Zotti T, Uva A, Ferravante A, Vessichelli M, Scudiero I, Ceccarelli M, Vito P, Stilo R. 2011. TRAF7 Protein Promotes Lys-29-linked Polyubiquitination of I κ B Kinase (IKK γ)/NF- κ B Essential Modulator (NEMO) and p65/RelA Protein and Represses NF- κ B Activation. *J Biol Chem* 286:22924–22933.

29. Wang J, Zhong X, Yin H. 2023. TRAF6 initiates inflammatory signaling via organizing membraneless cytoplasmic condensates. bioRxiv
<https://doi.org/10.1101/2023.06.19.545655>.

30. Jumper J, Evans R, Pritzel A, Green T, Figurnov M, Ronneberger O, Tunyasuvunakool K, Bates R, Židek A, Potapenko A, Bridgland A, Meyer C, Kohl SAA, Ballard AJ, Cowie A, Romera-Paredes B, Nikolov S, Jain R, Adler J, Back T, Petersen S, Reiman D, Clancy E, Zielinski M, Steinegger M, Pacholska M, Berghammer T, Bodenstein S, Silver D, Vinyals O, Senior AW, Kavukcuoglu K, Kohli P, Hassabis D. 2021. Highly accurate protein structure prediction with AlphaFold. 7873. *Nature* 596:583–589.

31. Simm D, Hatje K, Kollmar M. 2015. Waggawagga: comparative visualization of coiled-coil predictions and detection of stable single α -helices (SAH domains). *Bioinformatics* 31:767–769.
32. Finethy R, Coers J. 2016. Sensing the enemy, containing the threat: cell-autonomous immunity to *Chlamydia trachomatis*. *FEMS Microbiol Rev* 40:875–893.
33. Olive AJ, Haff MG, Emanuele MJ, Sack LM, Barker JR, Elledge SJ, Starnbach MN. 2014. *Chlamydia trachomatis*-Induced Alterations in the Host Cell Proteome Are Required for Intracellular Growth. *Cell Host & Microbe* 15:113–124.
34. Pruneda JN, Bastidas RJ, Bertsoulaki E, Swatek KN, Santhanam B, Clague MJ, Valdivia RH, Urbé S, Komander D. 2018. A *Chlamydia* effector combining deubiquitination and acetylation activities induces Golgi fragmentation. *Nat Microbiol* 3:1377–1384.
35. Le Negrate G, Krieg A, Faustin B, Loeffler M, Godzik A, Krajewski S, Reed JC. 2008. ChlaDub1 of *Chlamydia trachomatis* suppresses NF- κ B activation and inhibits I κ B α ubiquitination and degradation. *Cellular Microbiology* 10:1879–1892.
36. Sixt BS, Bastidas RJ, Finethy R, Baxter RM, Carpenter VK, Kroemer G, Coers J, Valdivia RH. 2017. The *Chlamydia trachomatis* Inclusion Membrane Protein CpoS Counteracts STING-Mediated Cellular Surveillance and Suicide Programs. *Cell Host & Microbe* 21:113–121.
37. Meier K, Jachmann LH, Türköz G, Babu Sait MR, Pérez L, Kepp O, Valdivia RH, Kroemer G, Sixt BS. 2023. The *Chlamydia* effector CpoS modulates the inclusion microenvironment and restricts the interferon response by acting on Rab35. *mBio* 14:e03190-22.

38. Huang J-P, Yang Y-X, Chen T, Wang D-D, Li J, Xu L-G. 2023. TRAF7 negatively regulates the RLR signaling pathway by facilitating the K48-linked ubiquitination of TBK1. *Virology* 38:419–428.
39. Liu Y. 2019. Defining the Roles of STING and TRAF7 in the Type I Interferon Antiviral Response. ProQuest Dissertations and Theses. Ph.D. McGill University (Canada), Canada -- Quebec, CA.
40. Tsitsikov EN, Phan KP, Liu Y, Tsytsykova AV, Kinter M, Selland L, Garman L, Griffin C, Dunn IF. 2023. TRAF7 is an essential regulator of blood vessel integrity during mouse embryonic and neonatal development. *iScience* 26:107474.
41. Ye J, Liu W, Yu X, Wu L, Chen Z, Yu Y, Wang J, Bai S, Zhang M. 2023. TRAF7-targeted HOXA5 acts as a tumor suppressor in prostate cancer progression and stemness via transcriptionally activating SPRY2 and regulating MEK/ERK signaling. *Cell Death Discov* 9:378.
42. Zadora PK, Chumduri C, Imami K, Berger H, Mi Y, Selbach M, Meyer TF, Gurumurthy RK. 2019. Integrated Phosphoproteome and Transcriptome Analysis Reveals Chlamydia-Induced Epithelial-to-Mesenchymal Transition in Host Cells. *Cell Reports* 26:1286-1302.e8.
43. Bueno R, Stawiski EW, Goldstein LD, Durinck S, De Rienzo A, Modrusan Z, Gnad F, Nguyen TT, Jaiswal BS, Chirieac LR, Sciaranghella D, Dao N, Gustafson CE, Munir KJ, Hackney JA, Chaudhuri A, Gupta R, Guillory J, Toy K, Ha C, Chen YJ, Stinson J, Chaudhuri S, Zhang N, Wu TD, Sugarbaker DJ, de Sauvage FJ, Richards WG, Seshagiri S. 2016. Comprehensive genomic analysis of malignant pleural

mesothelioma identifies recurrent mutations, gene fusions and splicing alterations. *Nat Genet* 48:407–16.

44. Stevers M, Rabban JT, Garg K, Ziffle JV, Onodera C, Grenert JP, Yeh I, Bastian BC, Zaloudek C, Solomon DA. 2019. Well-differentiated papillary mesothelioma of the peritoneum is genetically defined by mutually exclusive mutations in TRAF7 and CDC42. *Modern Pathology* 32:88–99.

45. Goode B, Joseph NM, Stevers M, Van Ziffle J, Onodera C, Talevich E, Grenert JP, Yeh I, Bastian BC, Phillips JJ, Garg K, Rabban JT, Zaloudek C, Solomon DA. 2018. Adenomatoid tumors of the male and female genital tract are defined by TRAF7 mutations that drive aberrant NF- κ B pathway activation. *Modern Pathology* 31:660–673.

46. Dermawan JK, Villafania L, Bale T, Singer S, D'Angelo SP, Tap WD, Antonescu CR. 2023. TRAF7-mutated Fibromyxoid Spindle Cell Tumors Are Associated With an Aggressive Clinical Course and Harbor an Undifferentiated Sarcoma Methylation Signature: A Molecular and Clinicopathologic Study of 3 Cases. *The American Journal of Surgical Pathology* 47:270.

47. Klein CJ, Wu Y, Jentoft ME, Mer G, Spinner RJ, Dyck PJB, Dyck PJ, Mauermann ML. 2017. Genomic analysis reveals frequent TRAF7 mutations in intraneural perineuriomas. *Annals of Neurology* 81:316–321.

48. Mishra-Gorur K, Barak T, Kaulen LD, Henegariu O, Jin SC, Aguilera SM, Yalbir E, Goles G, Nishimura S, Miyagishima D, Djenoune L, Altinok S, Rai DK, Viviano S, Prendergast A, Zerillo C, Ozcan K, Baran B, Sencar L, Goc N, Yarman Y, Ercan-Sencicek AG, Bilguvar K, Lifton RP, Moliterno J, Louvi A, Yuan S, Deniz E, Brueckner M,

Gunel M. 2023. Pleiotropic role of TRAF7 in skull-base meningiomas and congenital heart disease. *Proceedings of the National Academy of Sciences* 120:e2214997120.

49. Clark VE, Erson-Omay EZ, Serin A, Yin J, Cotney J, Özdoğan K, Avşar T, Li J, Murray PB, Henegariu O, Yilmaz S, Günel JM, Carrión-Grant G, Yılmaz B, Grady C, Tanrikulu B, Bakırcıoğlu M, Kaymakçalan H, Caglayan AO, Sencar L, Ceyhun E, Atik AF, Bayri Y, Bai H, Kolb LE, Hebert RM, Omay SB, Mishra-Gorur K, Choi M, Overton JD, Holland EC, Mane S, State MW, Bilgüvar K, Baehring JM, Gutin PH, Piepmeier JM, Vortmeyer A, Brennan CW, Pamir MN, Kılıç T, Lifton RP, Noonan JP, Yasuno K, Günel M. 2013. Genomic Analysis of Non-NF2 Meningiomas Reveals Mutations in TRAF7, KLF4, AKT1, and SMO. *Science* 339:1077–1080.

50. Reuss DE, Piro RM, Jones DTW, Simon M, Ketter R, Kool M, Becker A, Sahm F, Pusch S, Meyer J, Hagenlocher C, Schweizer L, Capper D, Kickingeder P, Mucha J, Koelsche C, Jäger N, Santarius T, Tarpey PS, Stephens PJ, Andrew Futreal P, Wellenreuther R, Kraus J, Lenartz D, Herold-Mende C, Hartmann C, Mawrin C, Giese N, Eils R, Collins VP, König R, Wiestler OD, Pfister SM, von Deimling A. 2013. Secretory meningiomas are defined by combined KLF4 K409Q and TRAF7 mutations. *Acta Neuropathol* 125:351–358.

51. Yang J, Lin Y, Guo Z, Cheng J, Huang J, Deng L, Liao W, Chen Z, Liu Z, Su B. 2001. The essential role of MEKK3 in TNF-induced NF- κ B activation. *Nature Immunology* 2:620–624.

52. Paudel R, Fusi L, Schmidt M. 2021. The MEK5/ERK5 Pathway in Health and Disease. *14. International Journal of Molecular Sciences* 22:7594.

53. Elwell CA, Jiang S, Kim JH, Lee A, Wittmann T, Hanada K, Melancon P, Engel JN. 2011. Chlamydia trachomatis Co-opts GBF1 and CERT to Acquire Host Sphingomyelin for Distinct Roles during Intracellular Development. *PLOS Pathogens* 7:e1002198.
54. Jäger S, Cimermancic P, Gulbahce N, Johnson JR, McGovern KE, Clarke SC, Shales M, Mercenne G, Pache L, Li K, Hernandez H, Jang GM, Roth SL, Akiva E, Marlett J, Stephens M, D'Orso I, Fernandes J, Fahey M, Mahon C, O'Donoghue AJ, Todorovic A, Morris JH, Maltby DA, Alber T, Cagney G, Bushman FD, Young JA, Chanda SK, Sundquist WI, Kortemme T, Hernandez RD, Craik CS, Burlingame A, Sali A, Frankel AD, Krogan NJ. 2011. Global landscape of HIV-human protein complexes. *Nature* 481:365–370.
55. Blonska M, You Y, Geleziunas R, Lin X. 2004. Restoration of NF- κ B Activation by Tumor Necrosis Factor Alpha Receptor Complex-Targeted MEKK3 in Receptor-Interacting Protein-Deficient Cells. *Molecular and Cellular Biology* 24:10757–10765.
56. Cox J, Mann M. 2008. MaxQuant enables high peptide identification rates, individualized p.p.b.-range mass accuracies and proteome-wide protein quantification. *Nat Biotechnol* 26:1367–1372.
57. Lupas A, Van Dyke M, Stock J. 1991. Predicting Coiled Coils from Protein Sequences. *Science* 252:1162–1164.
58. Käll L, Krogh A, Sonnhammer ELL. 2004. A combined transmembrane topology and signal peptide prediction method. *J Mol Biol* 338:1027–1036.
59. Vizcaíno JA, Deutsch EW, Wang R, Csordas A, Reisinger F, Ríos D, Dianes JA, Sun Z, Farrah T, Bandeira N, Binz P-A, Xenarios I, Eisenacher M, Mayer G, Gatto L,

Campos A, Chalkley RJ, Kraus H-J, Albar JP, Martinez-Bartolomé S, Apweiler R, Omenn GS, Martens L, Jones AR, Hermjakob H. 2014. ProteomeXchange provides globally coordinated proteomics data submission and dissemination. *Nat Biotechnol* 32:223–226.

60. Perez-Riverol Y, Csordas A, Bai J, Bernal-Llinares M, Hewapathirana S, Kundu DJ, Inuganti A, Griss J, Mayer G, Eisenacher M, Pérez E, Uszkoreit J, Pfeuffer J, Sachsenberg T, Yilmaz S, Tiwary S, Cox J, Audain E, Walzer M, Jarnuczak AF, Ternent T, Brazma A, Vizcaíno JA. 2019. The PRIDE database and related tools and resources in 2019: improving support for quantification data. *Nucleic Acids Res* 47:D442–D450.

61. Madeira F, Pearce M, Tivey ARN, Basutkar P, Lee J, Edbali O, Madhusoodanan N, Kolesnikov A, Lopez R. 2022. Search and sequence analysis tools services from EMBL-EBI in 2022. *Nucleic Acids Res* 50:W276–W279.

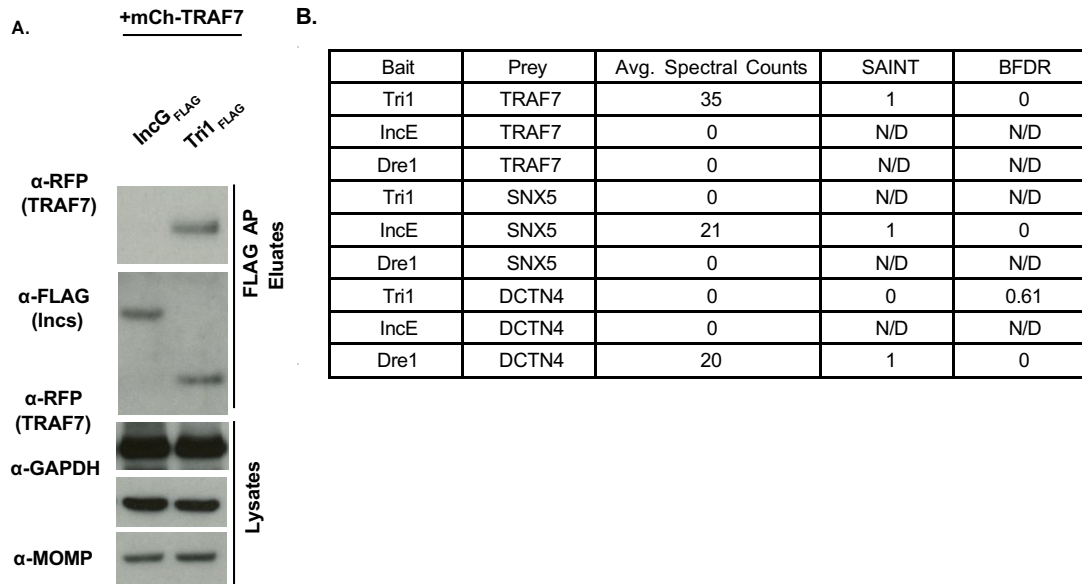


Figure 2.1. Tri1 and TRAF7 interact during infection. A. HeLa cells were transiently transfected with mCh-TRAF7 for 24 hrs and then infected with L2+pIncG_{FLAG} or L2+pTri1_{FLAG} for 24 hrs in the presence of inducer (aTc). Shown are the lysates and FLAG-bead affinity purified eluates immunoblotted with the indicated antibodies. GAPDH serves as a loading control and MOMP (Chlamydia Major Outer Membrane Protein) serves as a control for the efficiency of infection. B. FLAG-bead affinity purified eluates prepared from HeLa cells infected with L2 expressing the indicated Incs (pTri1_{FLAG}, pIncE_{FLAG}, or pDre1_{FLAG}) in the presence of inducer (aTc) were analyzed by LC/MS-MS. Shown are selected average spectral counts from biological triplicates, SAINT scores and BFDR (Bayesian False Discovery Rate). SAINT scores closer to 1 with a BFDR ≤ 0.05 suggests a high confidence interaction. N/D, not determined because no spectral counts were recorded. SNX5, Sorting nexin 5. DCTN4, Dynactin 4.

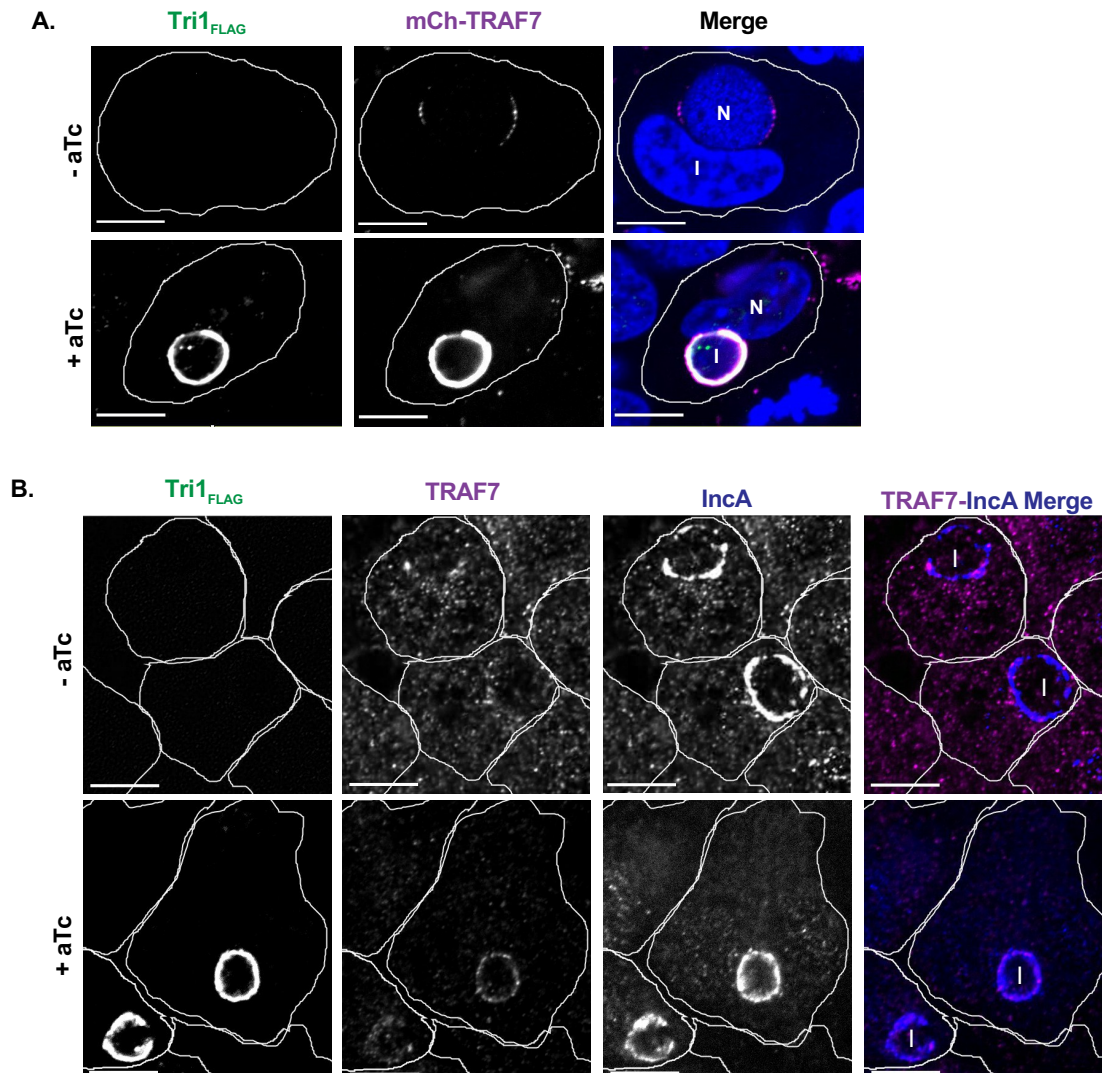


Figure 2.2. TRAF7 is recruited to the inclusion. A. Confocal immunofluorescence microscopy of HeLa cells transfected with mCh-TRAF7 for 24 hrs and then infected with L2+pTri1_{FLAG} for 24 hrs with or without aTc induction. Cells were fixed and stained with α -FLAG to visualize Tri1_{FLAG}. Merged images show mCh-TRAF7 (pseudo-colored magenta), Tri1_{FLAG} (pseudo-colored green), and DAPI (blue) staining. B. Confocal Immunofluorescence microscopy of HeLa cells infected with L2+pTri1_{FLAG} for 24 hrs with or without aTc induction. Cells were fixed and stained with antibodies to FLAG (to detect Tri1), TRAF7 (pseudo-colored magenta in merge), and IncA (blue in merge, to delineate the inclusion membrane). The merge panel only includes TRAF7 and IncA. The small amount of transfected mCh-TRAF7 present at the inclusion in the absence of inducer likely represents recruitment by chromosomally encoded Tri1. Shown are single z-slices. I, inclusion. N, nucleus. Scale bar = 10 μ m. Cell outlines are included for clarity.

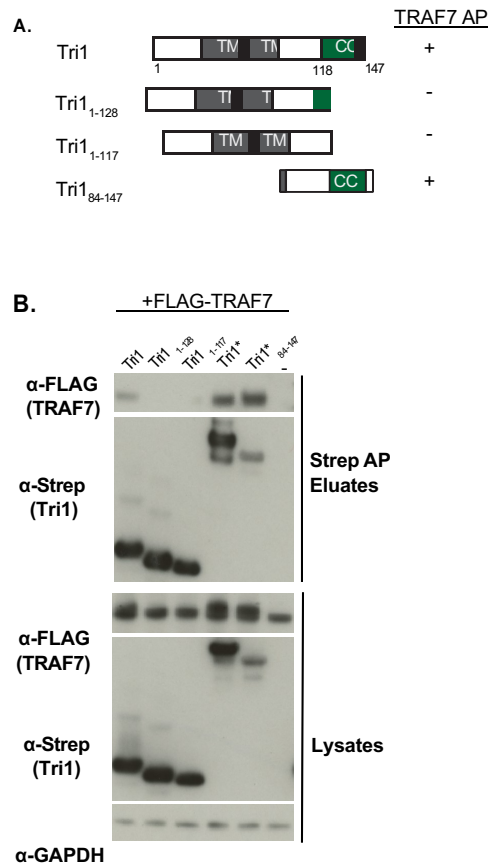


Figure 2. 3. The coiled-coil domain of Tri1 interacts with TRAF7. A. Schematic of Strep-tagged Tri1 variants. Variants that interact with TRAF7 are indicated with a "+" sign and variants that don't interact are indicated with a "-" sign. B. Lysates and eluates from affinity purifications of HEK293T cells co-transfected with the indicated Tri1-Strep or Strep-sfGFP-tagged variants (indicated with *) and with FLAG-TRAF7 and immunoblotted with the indicated antibodies. Control condition in which cells are transfected only with FLAG-TRAF7 is designated "-." GAPDH serves as a loading control for the lysates. Only Tri1 variants containing a complete coiled-coil domain (Tri1- Strep, Tri1- Strep-sfGFP and Tri1₈₄₋₁₄₇- Strep-sfGFP) co-AP'd with TRAF7.

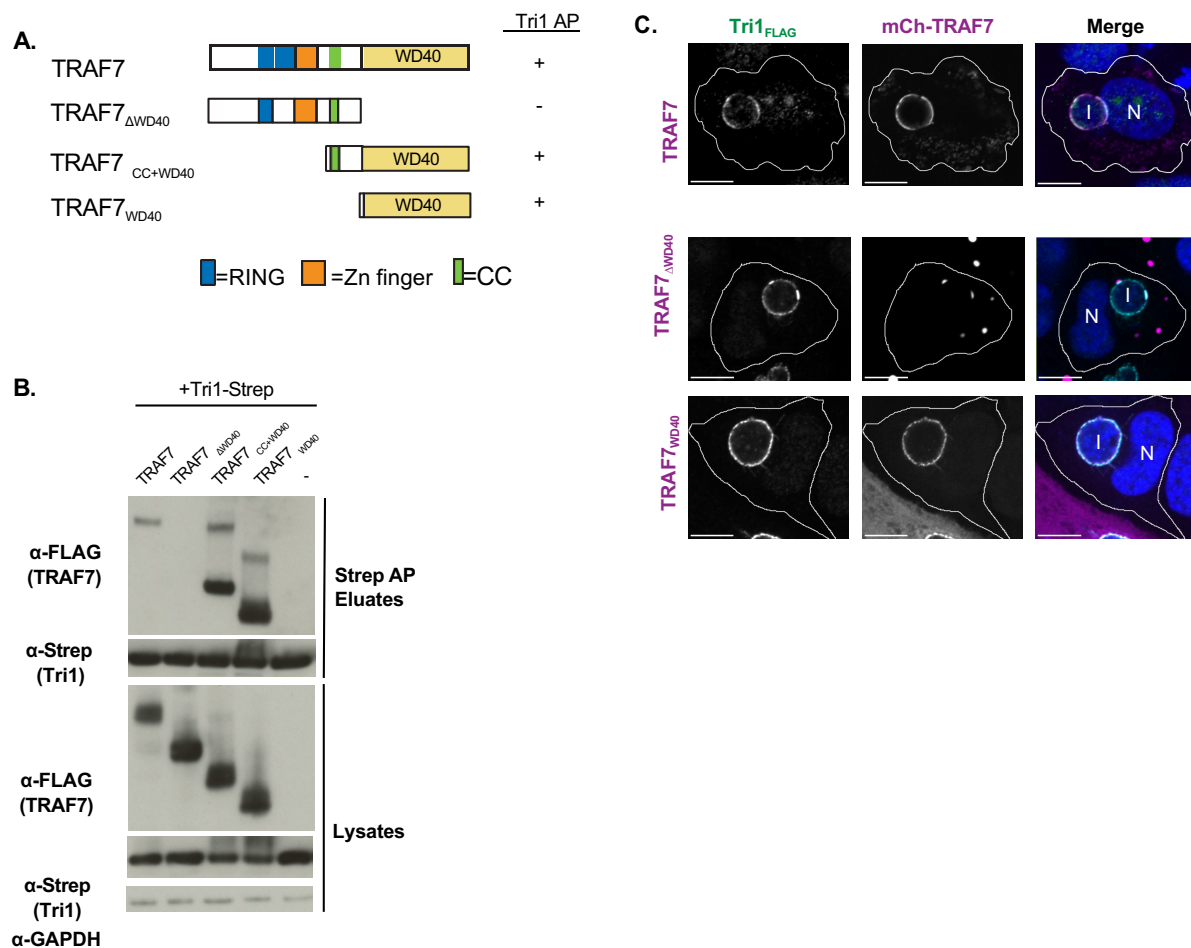


Figure 2. 4. The WD40 of TRAF7 is necessary and sufficient to interact with Tri1.

A. Schematic of TRAF7 constructs. Zn, zinc. CC, coiled-coil. RING, RING finger ubiquitin ligase domain. Variants that interact with TRAF7 are indicated with a "+" sign and variants that don't interact are indicated with a "-" sign. B. Lysates and eluates of HEK293T cells co-transfected with Tri1-Strep and the indicated FLAG-TRAF7 variants ("- " indicates the control with no TRAF7 added) were affinity purified with Strep-Tactin beads and immunoblotted with the indicated antibodies. GAPDH serves as a loading control for lysates. Only variants containing the WD40 domain of TRAF7 co-affinity purified with Tri1. The slower migrating band present in some of the TRAF7 samples likely represents stable dimers. C. Confocal Immunofluorescence microscopy of HeLa cells transfected with the indicated mCh-TRAF7 variants for 24 hrs followed by infection L2+pTri1_{FLAG} in the presence of aTc for 24 hrs. Cells were fixed and stained with α-FLAG and DAPI and imaged by confocal microscopy. Cell membranes are outlined. Shown are single z-slices. Scale bar = 10 μm. I, inclusion. N, nucleus.

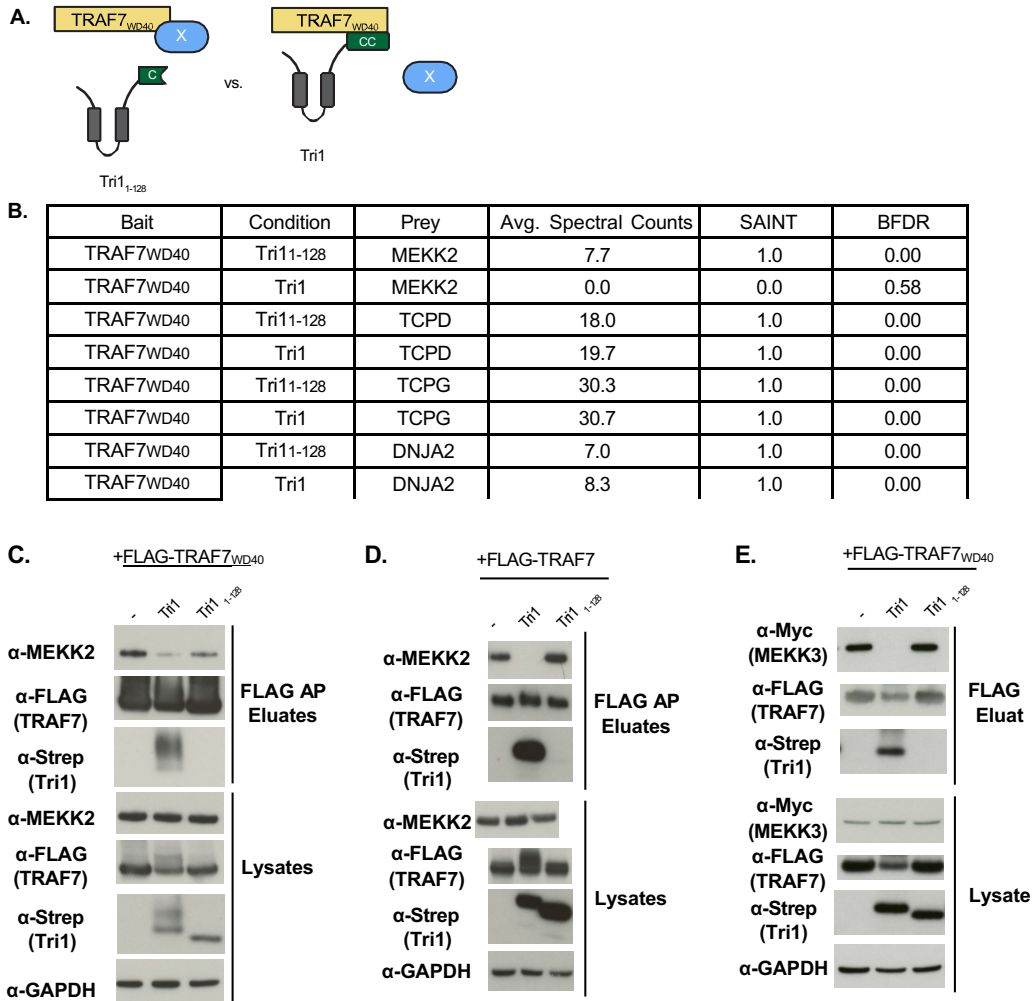


Figure 2.5. Tri1 displaces MEKK2 and MEKK3 binding to TRAF7. A. Schematic of displacement AP-MS analysis with a potential displaced TRAF7 native interactor represented by “X.” B. HEK293T cells co-transfected with FLAG-TRAF7^{WD40} (bait) and either Tri1₁₋₁₂₈-Strep or Tri1-Strep. Lysates were affinity purified over FLAG beads and analyzed by LC/MS-MS. Shown are the average spectral counts from 3 biological replicates, SAINT scores and Bayesian False Discovery Rate (BFDR) of selected TRAF7^{WD40} interacting partners in the presence of Tri1₁₋₁₂₈-Strep or Tri1-Strep. SAINT scores closer to 1 with a BFDR ≤ 0.05 suggest a high confidence interaction. Tri1 displaces MEKK2 binding to TRAF7^{WD40} but not to TCPD, TCPG, or DNJA2. C, D, E. Validation of Tri1-mediated displacement of MEKK2 and MEKK3 binding to the TRAF7 WD40 domain by co-transfection studies. HEK293T cells were co-transfected with either Tri1-Strep or Tri1₈₄₋₁₄₇-Strep (C,D,E), FLAG-TRAF7^{WD40} (C, E), FLAG-TRAF7 (D), and Myc-MEKK3 (E). Cells only transfected with FLAG-TRAF7^{WD40} (C,E) and FLAG-TRAF7 (D) were designated “-” and served as a control. Lysates were affinity purified using FLAG beads and analyzed by immunoblot with the indicated antibodies. GAPDH serves as a loading control for the lysates. Full length Tri1, but not Tri1₁₋₁₂₈, disrupts TRAF7 binding to MEKK2 and to MEKK3.

CLUSTAL 0(1.2.4) multiple sequence alignment

```
Tri1 (Serovar D)  MSFVGDSPVPLRSYMPPEAPLVDSASKARVSCCSERIAVLALGILSILFIVTGAALFIGAGW  60
Tri1 (Serovar L2) MSFVGDSPVPLRSYMPPEAPLVDSASKARVSCCSERIAVLALGILSILFIVTGAALFIGAGW  60
                  *****
Tri1 (Serovar D)  TTLPMIDVVVTLVVFVGSVMLGAVLTRISSYGGEPKKVSLDRFVLENERQGF LDKQRLADI  120
Tri1 (Serovar L2) TTLPMINVVVTLVVFVGSVMLGAVLTRISGYGGEPKKVSLDRFVLENERQGF LDKQRLADI  120
                  *****:*****
Tri1 (Serovar D)  SKEEIALAKQQIEEEEKAILHSIFPND  147
Tri1 (Serovar L2) SKEEIALAKQQIEEEEKAILHSIFPND  147
                  *****
```

Figure S2. 1. Alignment of Tri1 from L2 serovar D. A. Clustal alignment(61) of Tri1 from *C. trachomatis* serovars D and L2. Key: * , identical residues. :, highly conserved residues, ., weakly conserved residues.

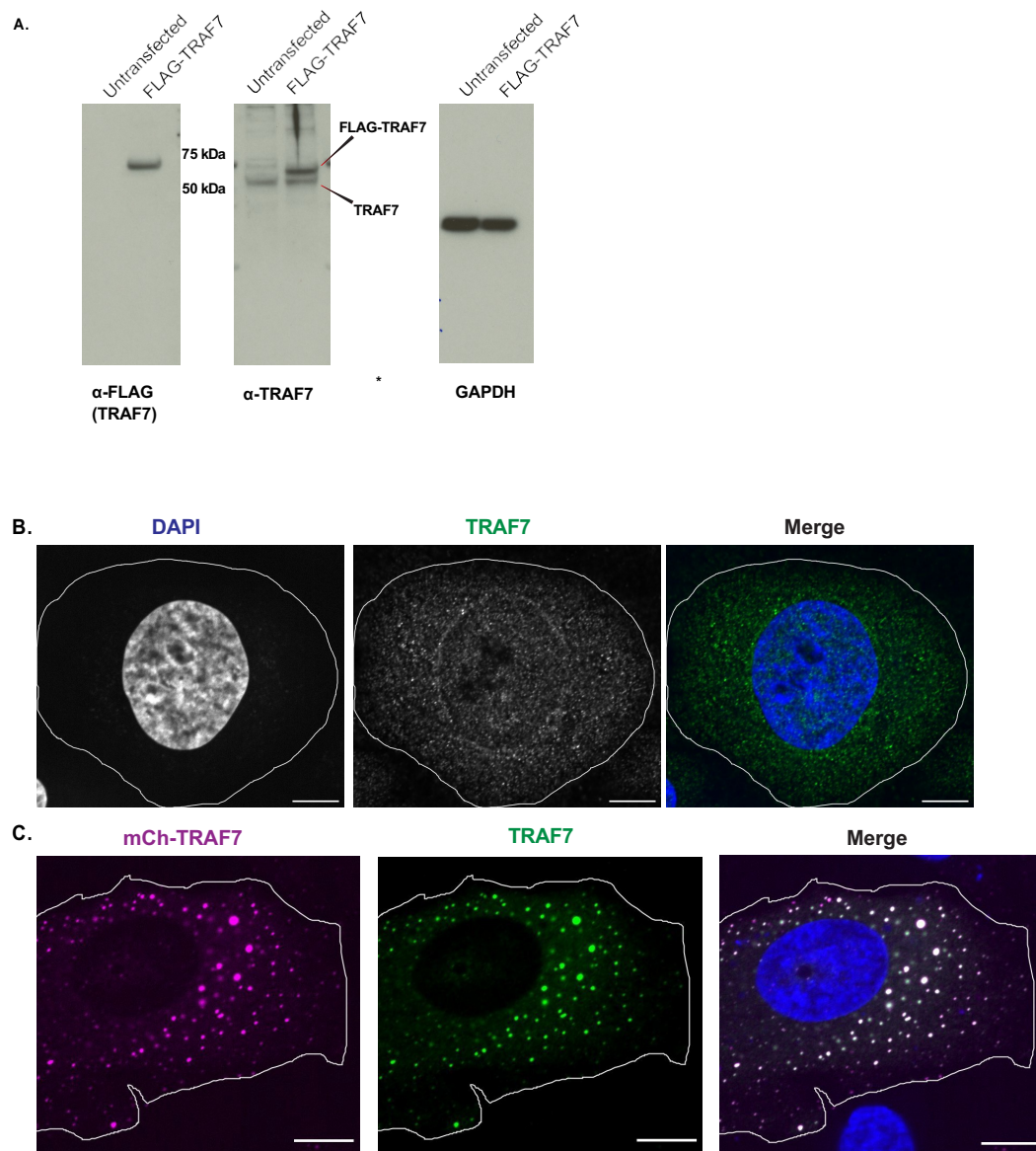


Figure S2.2. TRAF7 antibody detects endogenous TRAF7 and ectopically expressed TRAF7.

A. Lysates prepared from a HeLa cell line that only expresses TRAF7 isoform 2 (see materials and methods) that were either untransfected or transfected with FLAG-TRAF7 were immunoblotted with the indicated antibodies.

Antibodies to FLAG and TRAF7 detect similar sized proteins in the transfected lysates, which correspond with the predicted size of FLAG-TRAF7 (~78 kDa). The faster migrating band seen in the immunoblots probed with anti-TRAF7 represents endogenous TRAF7 isoform 2 (~67 kDa). GAPDH serves as a loading control. **B.** HeLa cells that were transfected with mCh-TRAF7 for 24 hrs were fixed and stained with anti-TRAF7 and DAPI and imaged by fluorescence confocal microscopy. **B.** Endogenous TRAF7 localizes to both the nucleus and cytosol. Cell membrane is outlined. Shown are Single z-slices. Scale bar = 10 μm .

CHAPTER 3 TRI1 ALTERS TRAF7 PROTEIN-PROTEIN INTERACTIONS

SUMMARY

We previously determined that Tri1 binds to the WD40 domain of TRAF7. This was interesting to us because this domain is known to form protein scaffolds in other proteins and has documented binding partners in the case of TRAF7. We thus wanted to test whether Tri1 through its interaction with TRAF7 can alter TRAF7 protein-protein interactions. We conducted quantitative AP-MS of transfected FLAG-TRAF7 and Tri1-Strep (either full-length (FL) or a non-TRAF7-binding variant in which the C-terminus is truncated) to discover host proteins whose binding to the TRAF7 WD40 domain is altered by Tri1 binding. Interestingly, we observed that Tri1 could both disrupt native TRAF7 interactions and promote novel TRAF7 protein-protein interactions. We overlaid the class of host proteins whose binding to TRAF7 increased in the presence of FL but not truncated Tri1 with predicted high confidence host protein interactors with Tri1 during *C. trachomatis* infection. We identified at least two classes of host proteins common to both data sets. We validated the prediction that one of these proteins, the nuclear importer protein IPO5, is recruited to the inclusion in a Tri1-dependent manner. Our analysis suggests that Tri1 may alter TRAF7-dependent signaling, both by disrupting native TRAF7 protein interactions such as MEKK2 and MEKK3, as well as by promoting new TRAF7 protein interactions with nuclear importer and exporter proteins.

INTRODUCTION

TRAF7 is a unique member of the tumor necrosis receptor associated factor (TRAF) family of proteins. Like many of the TRAFs, it encodes several protein domains, including a zinc finger domain, coiled-coil domain, and a RING finger domain, which is responsible for its ubiquitin ligase activity. Unlike the other TRAFs, TRAF7 encodes 7 WD40 repeats, which comprise its WD40 domain, at its C-terminus in place of a TRAF domain(1). The presence of this WD40 domain, a known protein scaffold domain(2), suggests that TRAF7 may participate in several protein-protein interactions. Indeed, TRAF7 was shown to interact with the mitogen activated kinase kinase kinase MEKK3 through its WD40 domain(3–5). However, the full range of TRAF7 protein-protein interactions remains to be revealed.

Our previous work (Chapter 2) demonstrated that the *C. trachomatis* Inc Tri1 can disrupt the interaction between TRAF7 and two of its native binding partners (MEKK2 and MEKK3). We expand on these observations by presenting a more comprehensive analysis of Tri1-dependent TRAF7 interactions identified using AP-MS of TRAF7 in the presence of Tri1 or a non-TRAF7-binding Tri1 variant (Tri1₁₋₁₂₈). Additionally, we compared this dataset to the Tri1_{FLAG} infection interactome (previously described in Chapter 2) and identified proteins common to both datasets, including the nuclear transport protein IPO5, which are of interest for future study(6). Through this approach, we determined that Tri1 may promote novel protein-protein interactions in addition to disrupting native TRAF7 interactions. Overall, this work highlights the potential role of Tri1 in modulating TRAF7 binding.

RESULTS

In preliminary experiments, we determined that Tri1-GFP (a *Chlamydia* serovar D construct expressing only the C-terminus which was a gift from the Valdivia lab) and mCh-TRAF7 co-localize during transfection (Fig 3.1). During transfection, TRAF7 localized to the nucleus, cytosol, and to puncta as previously reported (3, 7, 8). This was most clear in the case of full length TRAF7, which appears to localize to punctate structures within cells (Fig 3.1). In contrast, the WD40 domain of TRAF7 exhibited a more diffuse localization, appearing evenly spread out through the nucleus and cytosol.

To determine whether TRAF7 protein interactions are altered by Tri1, we performed AP-MS of transfected FLAG-TRAF7 (either full-length (FL) or the WD40 domain) in the presence of transfected Tri1-Strep or Tri1₁₋₁₂₈-Strep (the latter fails to bind either TRAF7_{FL} or TRAF7_{WD40}) (Fig. 3.2). We compared spectral counts for all TRAF7-binding proteins identified and computed a Log₂ fold-change (Log₂FC) for the following conditions (i) TRAF7_{FL} + Tri1 vs TRAF7 + Tri1₁₋₁₂₈ and (ii) TRAF7_{WD40} + Tri1 and TRAF7_{WD40} + Tri1₁₋₁₂₈. Positive Log₂FC values > 0.4 defined host proteins whose interactions with TRAF7_{FL} or TRAF7_{WD40} was dependent upon the ability of Tri1 to bind to the TRAF7_{FL} or TRAF7_{WD40}, respectively. This class of proteins may represent new TRAF7 interactions facilitated by Tri1. Negative Log₂FC values of < -0.4 defined host proteins whose interactions with TRAF7_{FL} or TRAF7_{WD40} was disrupted upon the ability of Tri1 to bind to the TRAF7_{FL} or TRAF7_{WD40}, respectively. This class of proteins defines native TRAF7 interactors that may be displaced by Tri1 (Fig 3.2). Only Log₂FC values with a p value less than or equal to 0.05 were considered in this analysis. A comparison

of the types of interactions found revealed that most of the interactions identified were enhanced interactions as opposed to disrupted (Fig. 3.2 G, H).

To further validate the class of host proteins whose interaction with TRAF7 was enhanced by Tri1, we compared the set of Tri1-enhanced proteins common to both TRAF7_{FL} and TRAF7_{WD40} with host proteins that co-affinity purified with FLAG-Tri1 expressing *C. trachomatis*-infected HeLa cells (“infection interactome”). A comparison of these datasets revealed 79 proteins that were unique to the TRAF7 dataset and 44 that were unique to the Tri1 infection dataset. Importantly, this analysis identified 8 proteins present in both the Tri1-dependent TRAF7 FL and TRAF7 WD40 data sets AND the Tri1-infection interactome, of which 7 are involved in protein transport. The eighth candidate protein, CAND1, is of interest because it is known to associate with E3 ligases to modulate their function(9, 10) and it was additionally identified as a potential TRAF7 binding partner by our collaborators David Solomon and Meredith Stevers. If Tri1 enhances the interaction of one or more of these eight proteins with TRAF7, we predict that these proteins should be recruited to the inclusion in a Tri1- and TRAF7- dependent manner. In preliminary experiments, we tested this hypothesis by examining the localization of the nuclear importer IPO5. (Fig 3.3 D,E). HeLa cells were transfected with fluorescently-tagged IPO5 (mIFP-IPO5) and infected with *C. trachomatis* expressing Tri1_{FLAG} from a plasmid. We found that IPO5 was recruited to the inclusion in a Tri1-dependent manner (Fig 3.4).

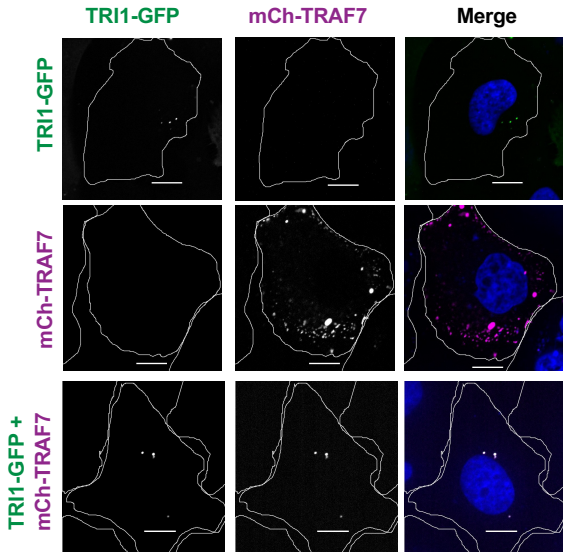


Figure 3. 1. Tri1 and TRAF7 co-localize at puncta during transfection. Confocal Immunofluorescence microscopy of HeLa cells transfected which were either individually transfected with Tri1-GFP (a C-terminal construct lacking transmembrane domains, top panels), mCh-TRAF7 (middle panels), or co-transfected with mCh-TRAF7 and Tri1-GFP for 24 hours. Cells were fixed and stained with DAPI and imaged by confocal microscopy. Tri1 is shown in green and mCh-TRAF7 in magenta (pseudocolored). Tri1-GFP localized to puncta in the absence and presence of mCh-TRAF7 transfection. During co-transfection, Tri1-GFP and mCh-TRAF7 co-localize at puncta. Cell membranes are outlined. Shown are single z-slices. Scale bar = 10 μ m. I, inclusion. N, nucleus.

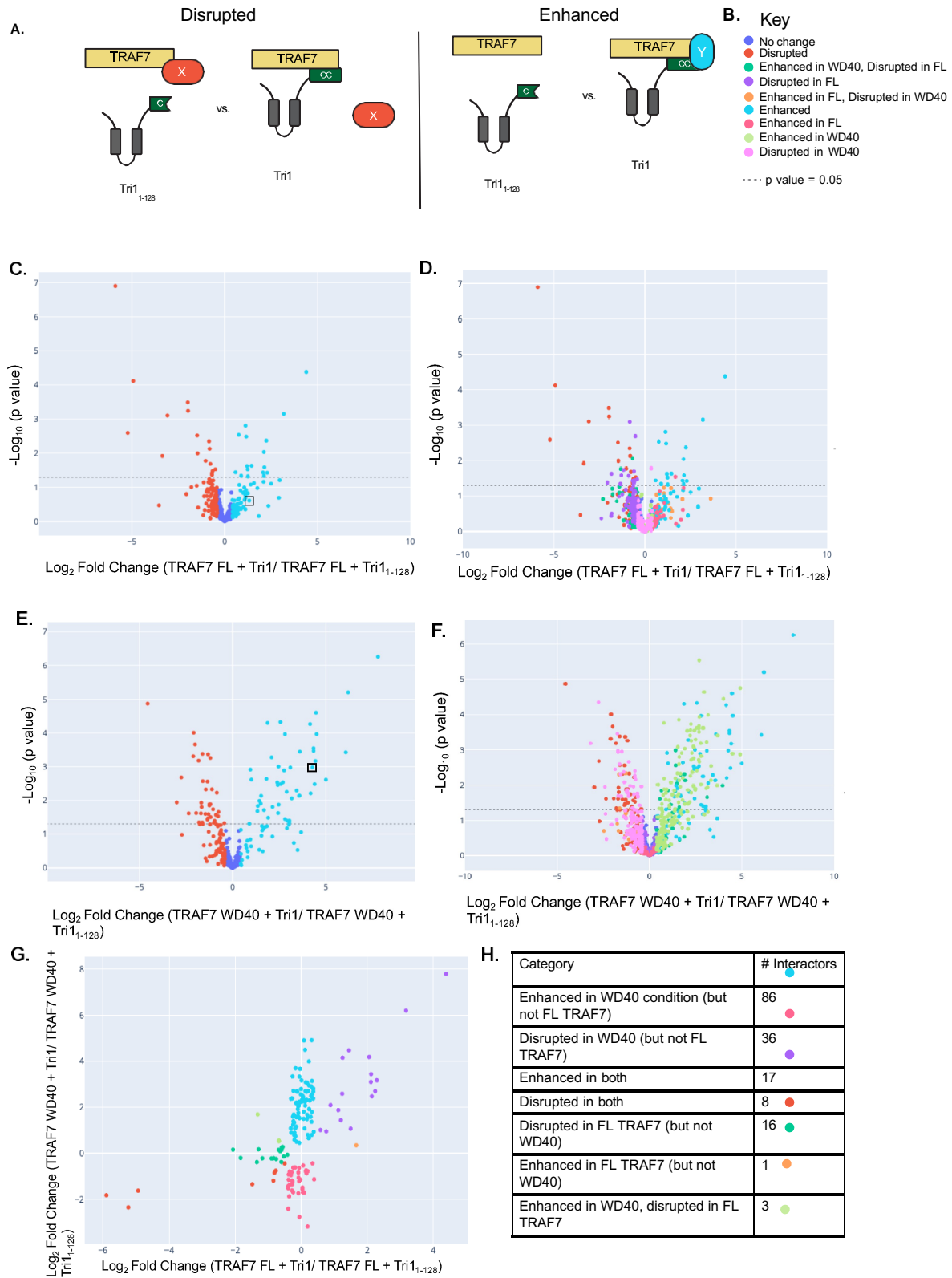


Figure 3. 2. Tri1 is predicted to modulate TRAF7 protein-protein interactions. A. Schematic of how Tri1 might displace (left cartoon) or enhance (right cartoon) binding of proteins to TRAF7 (figure continued on next page).

(Figure continued from previous page) C-F. Volcano plots of data from AP-MS analysis of the following: changes in peptide abundance (Log_2FC) between (i) TRAF7 FL + Tri1 and TRAF7+ Tri1₁₋₁₂₈ and (ii) TRAF7 WD40 + Tri1 and TRAF7 WD40+ Tri1₁₋₁₂₈ were used to identify enhanced and disrupted interactors. Log_2FC values greater than or equal to 0.4 are “enhanced” while those with values less than or equal to -0.4 are “disrupted.” Each dot represents an individual protein and is colored according to whether it is predicted to be enhanced or disrupted in the presence of Tri1 (see color key in B). Dotted horizontal line represents a p value of 0.05 for the Log_2FC and is the significance cut-off. C and D correspond to FL TRAF7 interactors while E and F correspond to TRAF7 WD40 interactors. G. Plot of Log_2FC of TRAF7 FL vs. TRAF7 WD40 altered proteins (see color key and numbers in H).

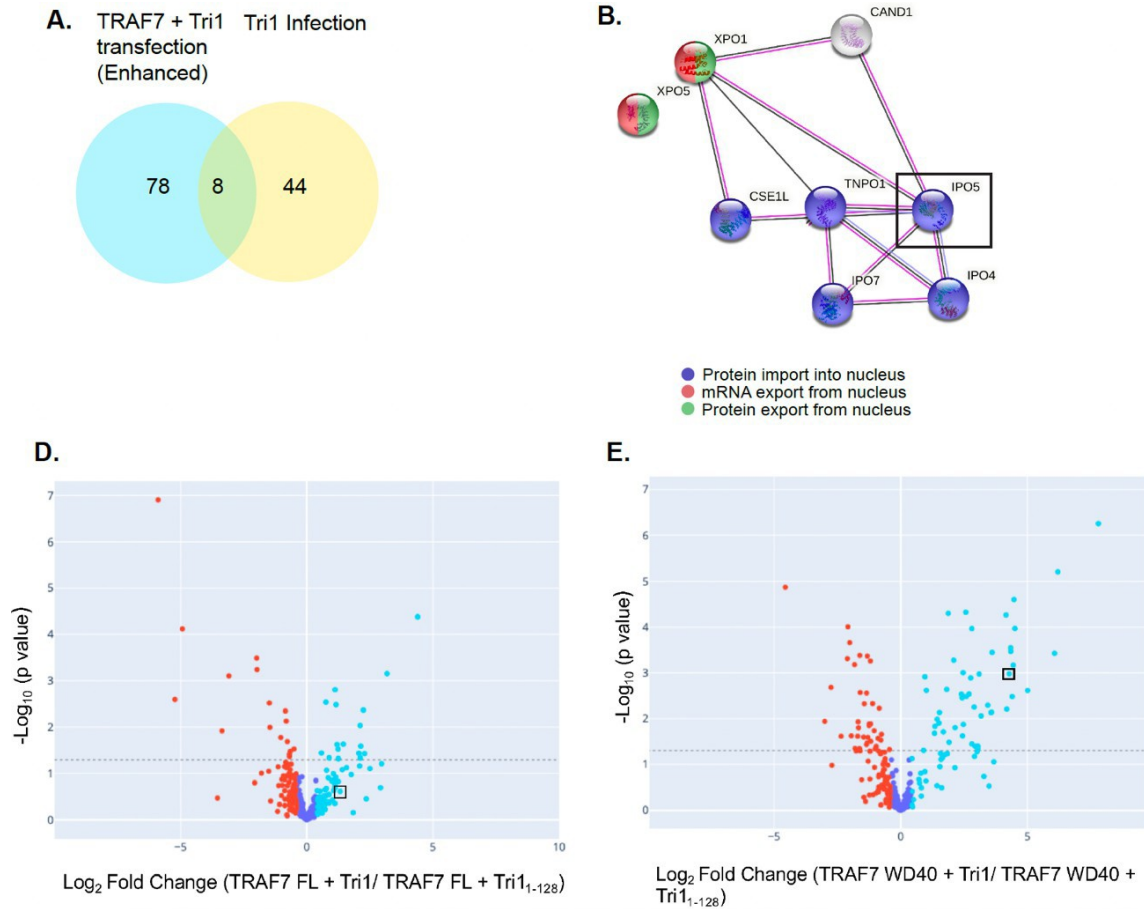


Figure 3. 3. Tri1 is predicted to promote TRAF7 interactions with transporter proteins during infection. A. Comparison of enhanced Tri1-dependent TRAF7 interactions during transfection and Tri1_{FLAG} infection interactors. B. STRING analysis of shared interactors in A reveals many of these proteins are involved in protein transport and may form complexes. IPO5 (boxed) was selected for further analysis). D and E. Volcano plots of TRAF7 AP-MS data with IPO5 boxed.

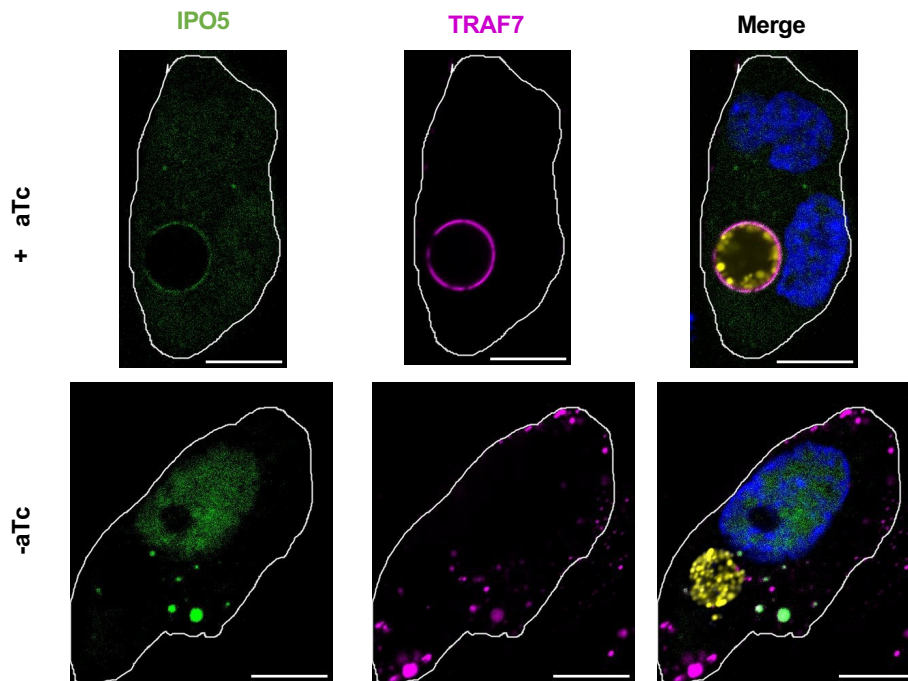


Figure 3. 4. IPO5 is recruited to the inclusion in a Tri1-dependent manner.

HeLa cells were transfected with mIFP-IPO5 (green) and mCh-TRAF7 (magenta) for 24 hrs prior to infection with L2 +pTri1_{FLAG} in the presence (+aTc) or absence (-aTc) of inducer. Cells were fixed and stained with DAPI (blue) and imaged by confocal microscopy. Shown are single z-slices. The outline of the HeLa is shown for clarity. Cells of interest are outlined. Nuclei are in blue, TRAF7 is in magenta, and bacteria are in yellow. Scale bar = 10 μ m.

DISCUSSION

Our analysis of the Tri1-dependent TRAF7 interactome reveals that Tri1 modulates TRAF7 protein-protein interactions by both disrupting native interactions and promoting novel complexes. Of the types of interactions identified, most were enhanced interactions as opposed to disrupted interactions, which suggests that Tri1 may promote novel TRAF7 functions during infection. We also detected many more enhanced interactions in the WD40 dataset compared to the full-length TRAF7 dataset. One explanation for this could be that full length TRAF7, according to microscopy observations, is more likely to form large aggregates. This may be due to the presence of a coiled-coil domain, which is necessary for TRAF7 oligomerization(3, 11). In contrast, the TRAF7 WD40 construct, which lacks this coiled-coil domain, does not aggregate and instead has diffuse localization throughout the cytosol and nucleus. This domain may thus have greater access to different proteins within the cell.

Additionally, we were excited to find overlap between this Tri1-dependent TRAF7 interactome dataset and the Tri1_{FLAG} infection interactome dataset. Because some of these interactions have not previously been observed for TRAF7, this overlap lends greater support to their relevance to infection. We found several nuclear import proteins in this dataset, including protein IPO5, which we confirmed can be recruited to the inclusion during infection. Additionally, the inclusion of the predicted enhanced interactor CAND1, a protein with roles in ubiquitin ligase activity(9, 12), in both datasets could indicate that Tri1 may alter TRAF7 ubiquitin ligase activity. Overall, we found that Tri1 may alter TRAF7 protein-protein interactions to both inhibit current TRAF7 functions and promote

novel functions. These studies may pave the way for uncovering novel functions of TRAF7.

MATERIALS AND METHODS

AP-MS

Methods to corresponding to AP-MS analysis are described in Chapter 2.

Fluorescence microscopy

Cells were seeded on coverslips, transfected using Effectene reagent, infected and fixed at 24 hpi and subsequently imaged at by confocal microscopy as described in Chapter 2.

ACKNOWLEDGEMENTS

We thank Danielle Swaney and Merve Cakir for their work on the bioinformatic analysis to produce quantitative (Log_2FC) comparisons of the TRAF7 AP-MS dataset. We also thank Kate Adams-Boone for her help with visualizing the AP-MS results and for generating volcano plots presented. We are also grateful to Meredith Stevers and David Solomon for their advice and their sharing of data, which allowed us to corroborate some of our results.

REFERENCES

1. Zotti T, Vito P, Stilo R. 2012. The seventh ring: Exploring TRAF7 functions. *Journal of Cellular Physiology* 227:1280–1284.
2. Xu C, Min J. 2011. Structure and function of WD40 domain proteins. *Protein Cell* 2:202–214.
3. Bouwmeester T, Bauch A, Ruffner H, Angrand PO, Bergamini G, Croughton K, Cruciat C, Eberhard D, Gagneur J, Ghidelli S, Hopf C, Huhse B, Mangano R, Michon AM, Schirle M, Schlegl J, Schwab M, Stein MA, Bauer A, Casari G, Drewes G, Gavin AC, Jackson DB, Joberty G, Neubauer G, Rick J, Kuster B, Superti-Furga G. 2004. A physical and functional map of the human TNF-alpha/NF-kappa B signal transduction pathway. *Nat Cell Biol* 6:97–105.
4. Xu L-G, Li L-Y, Shu H-B. 2004. TRAF7 Potentiates MEKK3-induced AP1 and CHOP Activation and Induces Apoptosis. *J Biol Chem* 279:17278–17282.
5. Tsitsikov EN, Phan KP, Liu Y, Tsytsykova AV, Kinter M, Selland L, Garman L, Griffin C, Dunn IF. 2023. TRAF7 is an essential regulator of blood vessel integrity during mouse embryonic and neonatal development. *iScience* 26:107474.
6. Zhang W, Lu Y, Li X, Zhang J, Lin W, Zhang W, Zheng L, Li X. 2019. IPO5 promotes the proliferation and tumorigenicity of colorectal cancer cells by mediating RASAL2 nuclear transportation. *Journal of Experimental & Clinical Cancer Research* 38:296.
7. Morita Y, Kanei-Ishii C, Nomura T, Ishii S. 2005. TRAF7 Sequesters c-Myb to the Cytoplasm by Stimulating Its Sumoylation. *Mol Biol Cell* 16:5433–5444.

8. Zotti T, Uva A, Ferravante A, Vessichelli M, Scudiero I, Ceccarelli M, Vito P, Stilo R. 2011. TRAF7 Protein Promotes Lys-29-linked Polyubiquitination of I κ B Kinase (IKK γ)/NF- κ B Essential Modulator (NEMO) and p65/RelA Protein and Represses NF- κ B Activation. *J Biol Chem* 286:22924–22933.
9. Chua YS, Boh BK, Ponyeam W, Hagen T. 2011. Regulation of Cullin RING E3 Ubiquitin Ligases by CAND1 In Vivo. *PLOS ONE* 6:e16071.
10. Shaaban M, Clapperton JA, Ding S, Kunzelmann S, Mäeots M-E, Maslen SL, Skehel JM, Enchev RI. 2023. Structural and mechanistic insights into the CAND1-mediated SCF substrate receptor exchange. *Molecular Cell* 83:2332-2346.e8.
11. Song X, Hu R, Chen Y, Xiao M, Zhang H, Wu S, Lu Q. 2024. The structure of TRAF7 coiled-coil trimer provides insight into its function in zebrafish embryonic development. *Journal of Molecular Cell Biology* mjad083.
12. Pierce NW, Lee JE, Liu X, Sweredoski MJ, Graham RLJ, Larimore EA, Rome M, Zheng N, Clurman BE, Hess S, Shan S, Deshaies RJ. 2013. Cand1 Promotes Assembly of New SCF Complexes through Dynamic Exchange of F Box Proteins. *Cell* 153:206–215.

CHAPTER 4 SELECT SIGNALING PATHWAYS ARE DEPENDENT ON TRI1
EXPRESSION DURING INFECTION

INTRODUCTION

TRAF7 is involved in several signaling pathways which may be relevant for *Chlamydia* infection, such as NF- κ B, JNK, and type I Interferon signaling(1–5). Additionally, our AP-MS analysis of Tri1 and TRAF7 during transfection suggest that Tri1 modulates the interaction between TRAF7 and several interactors by both displacing native interactors and by promoting novel TRAF7 protein-protein interactions (Chapters 2 and 3). To determine host cell pathways that may be affected by the Inc Tri1, we performed transcriptomics on A2EN cells infected with strains of *C. trachomatis* L2 in which Tri1 was conditionally depleted by CRISPRi.

RESULTS

To determine whether host gene expression was altered by Tri1, we infected A2EN cells for 24 hrs with strains of L2 in which Tri1 transcription is conditionally inhibited by CRISPRi. Specifically, we used L2 strains that had been previously transformed with a plasmid expressing Cas12 under the control of an aTc-inducible promoter and either expressing a constitutively expressed guide RNA targeting Tri1 or no guide RNA (a kind gift from Scot Ouellette, Elizabeth Rucks, and Natalie Sturd(6)). Uninfected cells (termed “mock infected”) served as an additional control. In all conditions cells were treated with aTc to induce Cas12 expression.

As it has previously been reported that Cas12 expression resulted in variability in progeny production, we first titrated aTc levels to optimize Cas12 expression while minimizing potential toxic effects of Cas12 (Figure 4.1A,B)(7). Having optimized these conditions, we next assessed whether Tri1 was depleted in A2EN cells infected with L2 expressing the CRISPRi vector containing inducible Cas12 and the Tri1 gRNA compared to A2EN cells infected with L2 expressing the CRISPRi-Cas12 vector without any gRNA. As we do not have an antibody that recognizes endogenous Tri1, we assessed Tri1 depletion by quantitative RT-PCR (qRT-PCR) of cells at 24 hours post infection. We found that depletion was successful, resulting in 95% Tri1 transcript reduction when targeted by CRISPRi (Figure 4.1C). We thus used the conditions of 0.5 nM aTc induction and 24 hpi for infection. Initial RNAseq analysis confirmed that no Tri1 transcripts were detected in the CRISPRi-targeted condition while transcripts were detected in the control CRISPRi infection condition. Additionally, RNAseq analysis did not identify individual host genes whose expression was significantly differentially expressed between cells expressing the

Tri1 CRISPRi and control CRISPRi datasets. However, gene set enrichment analysis (GSEA) revealed that six pathways were differentially expressed between the two conditions. Three pathways (androgen response, UV response, and interferon gamma response) were upregulated and three pathways were downregulated (apical junction, Myc targets V1, Myc targets and V2).

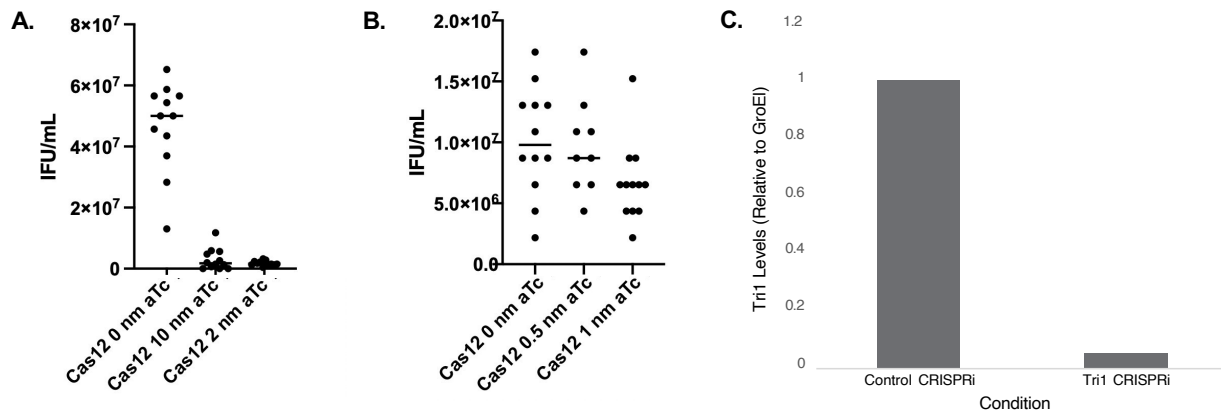
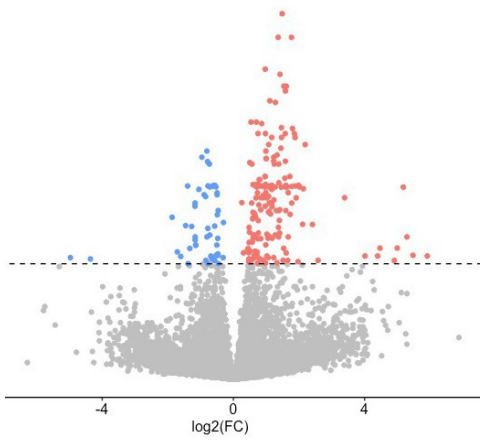
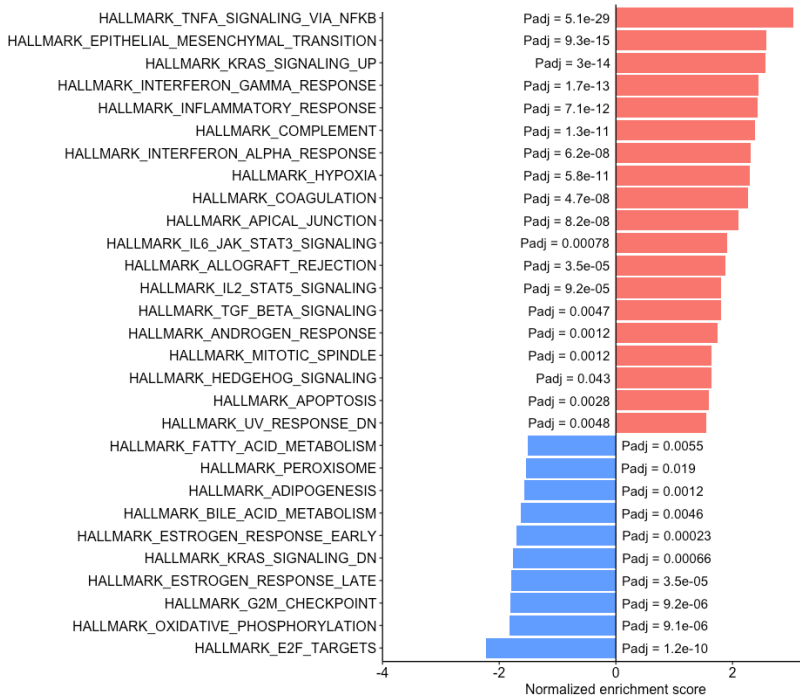


Figure 4. 1. Optimization of RNAseq conditions. Progeny assay results for *C. trachomatis* CRISPRi strain expressing inducible Cas12 under high (A) and low (B) aTc induction conditions. C. Results from qRT-PCR analysis of A2EN cells infected with either the control CRISPRi strain (expressing inducible Cas12 but no guide) or the Tri1 targeting CRISPRi strain at 24 hpi with 1 nM aTc for induction showed a 95% reduction of Tri1 transcript levels (relative to the *Chlamydia* gene GroEL to control for genome copy number) in the Tri1 targeting conditions.

A.



B.



C.

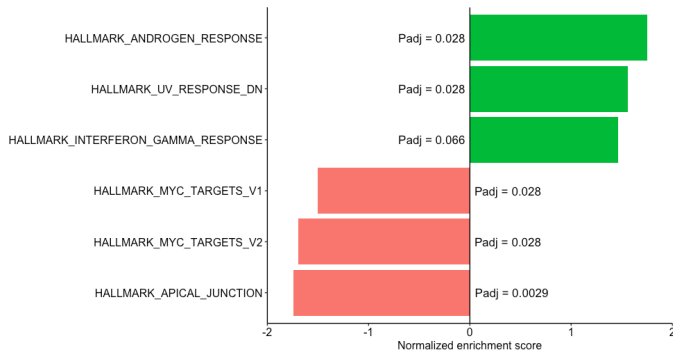


Figure 4. 2. GSEA of RNAseq results identifies Tri1-dependent pathways during infection. A. Volcano plot of genes significantly upregulated (red) or downregulated (blue) during infection with control CRISPRi strain infection (no guide RNA, figure continued on next page)

(figure continued from previous page) compared to mock infected cells. B. Gene set enrichment analysis (GSEA) comparison of control CRISPRi infection and mock infection reveals several pathways that are significantly altered upon Chlamydia infection. Red = upregulated upon infection. Blue = downregulated upon infection. C. GSEA of control CRISPRi and Tri CRISPRi infections identified 6 pathways that were dependent upon Tri1 expression. Green = upregulated during Tri1 depletion. Red = downregulated in the presence of endogenous Tri levels.

DISCUSSION

We initially predicted that Tri1 depletion would have significant consequences for cell signaling that would be noticeable by transcriptomic analysis. This was partly due to our previous findings that Tri1 can alter TRAF7 protein-protein interactions. However, we found that no transcripts were significantly altered in a Tri1-dependent manner.

Additional analysis through GSEA, a method developed to observe subtle transcriptional changes in datasets, revealed that multiple signaling pathways may be dependent on Tri1 expression. This result suggests that the effect of Tri1 on TRAF7 signaling during infection may be a subtle change.

MATERIALS AND METHODS

Cell culture

A2EN cells were obtained from American Type Culture Collection (ATCC) and cultured and maintained in Keratinocyte Media (Gibco) supplemented with 50 µg/mL Bovine Pituitary Extract (Gibco), 0.5 ng/mL Human Recombinant EGF (Gibco), and 10% (v/v) FBS at 37°C in 5% CO₂.

RNAseq methods

A2EN cells were seeded at 1.2x 10⁶ cells per well in 2 ml of keratinocyte media + 10% FBS in a 6-well plate, incubated overnight at 37 C and 5 % CO₂. One well of a 6-well plate was used for each condition (mock infected, Tri1 CRISPRi *C. trachomatis* L2 infected, control CRISPRi *C. trachomatis* L2 infected). 5 replicates were used per condition and duplicate wells were also seeded for each condition for later qRT-PCR validation of Tri1 KD. Cells were infected at an MOI of 1 by centrifugation at 1000 rpm for 30 min at 4 C prior to incubation at 37 C and 5 % CO₂ for 1.5 hrs. After the incubation, the infection media was removed and replaced with fresh media containing 1 nM aTc. At 24 hpi, cells were washed once with 1 mL PBS and either pelleted for RT-PCR analysis or lysed for RNAseq analysis. RNA isolation from pelleted cells was conducted using a Bio-Rad Aurum RT-PCR kit. RNA was then used to conduct one-step qRT-PCR using a Quant-X One-Step qRT-PCR TB Green Kit (Takara) using primers to Tri1 (forward primer: 5' CTTGCGCTCGGTATTCTTAGT 3', reverse primer 5' CAGGGTAACCACTACGTCAATC 3') or the *C. trachomatis* gene GroEL

(forward primer: 5' CGGCCGTCCTCTTCTTATTATAG 3', reverse primer 5' GGAGCTTTAACTGCGCAAAC 3') as a genome control.

Cell lysis was performed on ice with 500 μ L of Zymo DNA/RNA Shield (1X final in RNase free water), scraped, and transferred to microcentrifuge tubes. Lysate samples for RNAseq were then flash frozen and stored at -80 C for future processing. Lysate processing for RNAseq analysis was performed as previously described: "RNA was extracted from infected cells using the Zymo Pathogen Magbead Kit according to manufacturer's instructions. Following DNase treatment, human cytosolic and mitochondrial ribosomal DNA was depleted using FastSelect (Qiagen). RNA was then fragmented and underwent library preparing using the NEBNext Ultra II RNA-seq Kit (New England Biolabs). Libraries underwent paired-end sequencing on an Illumina NovaseqX. Differential expression analysis was performed in R (v.4.3.2) using the package limma-voom1 (v3.58.1). Significant genes were identified using a Benjamini-Hochberg false discovery rate (FDR) < 0.1. Gene set enrichment analysis (GSEA) was performed using the package fgsea (v1.28.0), and the Hallmark pathways were obtained from the package msigdb (v7.5.1). The t-statistics (obtained from limma's differential expression analysis) were used to rank all genes and used as input for the fgseaMultilevel function (minSize =15, maxSize = 500). Pathways with adjusted P-value below 0.05 were considered statistically significant (8)."

Progeny assays

For experiments assaying production of infectious progeny, primary infectious were performed at an MOI of 1 in A2EN cells using the infection protocol described above and with varying amounts of aTc to induce Cas12 expression for initial aTc titration tests. Infected A2EN cells were osmotically lysed in ddH₂O at 48 hpi for secondary infections. Secondary infections were conducted by infecting HeLa cells with 10-fold serial dilutions of primary infection harvests. Cells were infected as previously described, but after the removal of infection media, fresh media containing 1mg/mL Heparin (Sigma) was added to cells. At 24 hpi cells were fixed in 4% PFA in PBS for 15 minutes at room temperature and then permeabilized in 0.2% Triton X-100 in PBS for 15 minutes at room temperature. Cells were blocked in PBS containing 1% BSA for 1 hour and then stained with indicated primary and fluorophore-conjugated secondary antibodies in 1% BSA for 1 hour each. Coverslips were mounted on Vectashield mounting media with or without DAPI (Vector Laboratories) and imaged on laser scanning disc confocal microscope. Progeny production was then calculated after counting inclusion formation using FIJI software.

ACKNOWLEDGEMENTS

We thank members of the Langelier lab for performing RNA-sequencing analysis and conducting further bioinformatic analysis of these samples to identify Tri1-relevant pathways. Additionally, we thank Natalie Sturd and the Rucks and Ouellette, labs for sharing their Tri1-targeting CRISPRi strain and offering advice.

REFERENCES

1. Huang J-P, Yang Y-X, Chen T, Wang D-D, Li J, Xu L-G. 2023. TRAF7 negatively regulates the RLR signaling pathway by facilitating the K48-linked ubiquitination of TBK1. *Virology* 38:419–428.
2. Li PT, Li Y, Chen Y, Zhang JX, Luo ZH, Zhang YF, Jiang J, Wang YL, Zhang ZP, Jiang YH, Zou PF. 2023. Teleost TRAF7, a protein functions in the host antiviral responses via NF- κ B and IRF3/7 mediated signaling. *Frontiers in Marine Science* 10.
3. Zotti T, Scudiero I, Vito P, Stilo R. 2017. The Emerging Role of TRAF7 in Tumor Development. *J Cell Physiol* 232:1233–1238.
4. Bouwmeester T, Bauch A, Ruffner H, Angrand PO, Bergamini G, Croughton K, Cruciat C, Eberhard D, Gagneur J, Ghidelli S, Hopf C, Huhse B, Mangano R, Michon AM, Schirle M, Schlegl J, Schwab M, Stein MA, Bauer A, Casari G, Drewes G, Gavin AC, Jackson DB, Joberty G, Neubauer G, Rick J, Kuster B, Superti-Furga G. 2004. A physical and functional map of the human TNF- α /NF- κ B signal transduction pathway. *Nat Cell Biol* 6:97–105.
5. Xu LG, Li LY, Shu HB. 2004. TRAF7 potentiates MEKK3-induced AP1 and CHOP activation and induces apoptosis. *The Journal of biological chemistry* 279:17278–82.
6. Sturd NA, Wood MG, Durham L, Ouellette SP, Rucks EA. 2023. FLI1 localization to the chlamydial inclusion involves multiple mechanisms. preprint. *Microbiology*.
7. Ouellette SP, Blay EA, Hatch ND, Fisher-Marvin LA. CRISPR Interference To Inducibly Repress Gene Expression in *Chlamydia trachomatis*. *Infection and Immunity* 89:e00108-21.

8. 2024. Microbial Dynamics and Pulmonary Immune Responses in COVID-19 Secondary Bacterial Pneumonia. <https://www.researchsquare.com>. Retrieved 17 March 2024.

CHAPTER 5 CONCLUSIONS

In this work we employed proteomics, genetics, biochemistry, and confocal microscopy to evaluate the interaction between the *C. trachomatis* effector Tri1 and the host ubiquitin ligase TRAF7 during infection (Chapter 2). After identifying the regions responsible for this interaction and determining that Tri1 interacts with the TRAF7 WD40 domain, a known protein scaffolding domain, we decided to test whether Tri1 could alter TRAF7 protein-protein interactions. We hypothesized that Tri1 binding to TRAF7 could disrupt native TRAF7 protein-protein interactions, enhance existing interactions, or promote the formation of novel complexes. We tested these models using AP-MS and determined that Tri1 can both disrupt native TRAF7 interactions and promote novel interactions (Chapters 2 and 3). Our additional work on the predicted TRAF7 interactors confirmed that Tri1 can displace the native TRAF7 interactors MEKK2 and MEKK3 and that it can promote IPO5 localization at the inclusion (Chapters 2 and 3). Additionally, we used RNAseq analysis of cells infected with a *C. trachomatis* strain which allows for CRISPRi-mediated depletion of Tri1 to generate hypotheses about the role of the Tri1-TRAF7 complex during infection. We found that although no specific genes were significantly altered in a Tri1-dependent manner in cultured cells at 24 hpi, gene set enrichment analysis revealed that some pathways were significantly upregulated or downregulated upon Tri1 depletion (Chapter 4). Together, these results suggest that Tri1 can alter TRAF7 protein-protein interactions and potentially cell signaling.

Future work to further characterize the role of the Tri1-TRAF7 complex during infection will involve continued analysis of the several predicted Tri1-dependent TRAF7 protein-protein interactions. Of particular interest are the many interactions that are

promoted by Tri1, since they comprised a larger portion of the data and they could allow for the identification of novel TRAF7 functions. Future experiments will also be conducted to determine the effects of Tri1 displacement of MEKK2 and MEKK3 on TRAF7-dependent signaling. Because TRAF7 and MEKK2/3 can modulate several signaling pathways, the Tri1 RNAseq results can be used to guide which pathways to prioritize. Finally, to obtain a more complete picture of the role of TRAF7-Tri1 during infection, future studies should be conducted to measure changes in TRAF7 ubiquitin ligase activity during infection.

Overall, this thesis contributes to the growing body of work suggesting the important roles of Incs during *Chlamydia* infection. We present a biochemical characterization of the Tri1-TRAF7 interaction, which will be crucial to fully uncover its role in *C. trachomatis* survival and may pave the way for a more complete understanding of TRAF7 in cell signaling.

Publishing Agreement

It is the policy of the University to encourage open access and broad distribution of all theses, dissertations, and manuscripts. The Graduate Division will facilitate the distribution of UCSF theses, dissertations, and manuscripts to the UCSF Library for open access and distribution. UCSF will make such theses, dissertations, and manuscripts accessible to the public and will take reasonable steps to preserve these works in perpetuity.

I hereby grant the non-exclusive, perpetual right to The Regents of the University of California to reproduce, publicly display, distribute, preserve, and publish copies of my thesis, dissertation, or manuscript in any form or media, now existing or later derived, including access online for teaching, research, and public service purposes.

DocuSigned by:

90A5A50635D5404... Author Signature

3/20/2024
Date